Potential Molecular Mechanisms and Remdesivir Treatment for Acute Respiratory Syndrome Corona Virus 2 Infection/COVID 19 Through RNA Sequencing and Bioinformatics Analysis

Bioinformatics and Biology Insights
Volume 15: 1–15

DOI: 10.1177/11779322211067365
SAGE

G Prashanth[1], Basavaraj Vastrad[2], Chanabasayya Vastrad[3] and Shivakumar Kotrashetti[3]

[1]Department of General Medicine, Basaveshwara Medical College, Chitradurga, India. [2]Department of Biochemistry, Basaveshwar College of Pharmacy, Gadag, India. [3]Biostatistics and Bioinformatics, Chanabasava Nilaya, Dharwad, India.

ABSTRACT

INTRODUCTION: Severe acute respiratory syndrome corona virus 2 (SARS-CoV-2) infections (COVID 19) is a progressive viral infection that has been investigated extensively. However, genetic features and molecular pathogenesis underlying remdesivir treatment for SARS-CoV-2 infection remain unclear. Here, we used bioinformatics to investigate the candidate genes associated in the molecular pathogenesis of remdesivir-treated SARS-CoV-2-infected patients.

METHODS: Expression profiling by high-throughput sequencing dataset (GSE149273) was downloaded from the Gene Expression Omnibus, and the differentially expressed genes (DEGs) in remdesivir-treated SARS-CoV-2 infection samples and nontreated SARS-CoV-2 infection samples with an adjusted *P* value of <.05 and a |log fold change| > 1.3 were first identified by limma in R software package. Next, pathway and gene ontology (GO) enrichment analysis of these DEGs was performed. Then, the hub genes were identified by the NetworkAnalyzer plugin and the other bioinformatics approaches including protein-protein interaction network analysis, module analysis, target gene—miRNA regulatory network, and target gene—TF regulatory network. Finally, a receiver-operating characteristic analysis was performed for diagnostic values associated with hub genes.

RESULTS: A total of 909 DEGs were identified, including 453 upregulated genes and 457 downregulated genes. As for the pathway and GO enrichment analysis, the upregulated genes were mainly linked with influenza A and defense response, whereas downregulated genes were mainly linked with drug metabolism—cytochrome P450 and reproductive process. In addition, 10 hub genes (VCAM1, IKBKE, STAT1, IL7R, ISG15, E2F1, ZBTB16, TFAP4, ATP6V1B1, and APBB1) were identified. Receiver-operating characteristic analysis showed that hub genes (CIITA, HSPA6, MYD88, SOCS3, TNFRSF10A, ADH1A, CACNA2D2, DUSP9, FMO5, and PDE1A) had good diagnostic values.

CONCLUSION: This study provided insights into the molecular mechanism of remdesivir-treated SARS-CoV-2 infection that might be useful in further investigations.

KEYWORDS: SARS-CoV-2 infection, differentially expressed genes, pathway enrichment analysis, protein-protein interaction, ROC analysis

RECEIVED: September 16, 2021. **ACCEPTED:** November 29, 2021.

TYPE: Original Research

FUNDING: The author(s) received no financial support for the research, authorship, and/or publication of this article.

DECLARATION OF CONFLICTING INTERESTS: The author(s) declared no potential conflicts of interest with respect to the research, authorship, and/or publication of this article.

CORRESPONDING AUTHOR: Chanabasayya Vastrad, Biostatistics and Bioinformatics, Chanabasava Nilaya, Bharthinagar, Dharwad 580001, Karnataka, India. Email: channu.vastrad@gmail.com

Introduction

At the December of 2019, a novel corona virus, called severe acute respiratory syndrome corona virus 2 (SARS-CoV-2) or novel corona virus 2019 (2019-nCoV) is a single-stranded RNA, nonsegmented, enveloped viruses, resulted fast spreading from its origin in China to the rest of the globe.[1] Symptoms of this viral infection vary in severity from a simple cold to severe illness, and can lead to death. Despite the fact that great progress has been made in antivirals and vaccination for this SARS-CoV-2 infection, the survival rate is less. Remdesivir is the only antiviral drug for treatment of SARS-CoV-2 infection.[2] Because the precise molecular changes after remdesivir treatment for SARS-CoV-2 infection remain unknown, it is extremely essential to examine molecular changes during remdesivir treatment in SARS-CoV-2 infection.[3]

Expression profiling by high-throughput sequencing is very essential to understand the molecular pathogenesis of viral infection and also to the advancement of novel antivirals drugs and vaccines for the novel viral infections.[4] With the rapid advancement of next-generation sequencing (NGS) technology to find out differentially expressed genes (DEGs) during diagonosis of viral infections.[5] We rationally presume that DEGs can affect the promotion of various viral infections. Now, through expression profiling by high-throughput sequencing investigation using NGS technology, more and more DEGs were linked with SARS-CoV-2 infection during remdesivir treatment and understanding its biological characteristics is essential in improving clinical treatment outcomes.

In the current investigation, we downloaded the RNA-seq dataset GSE149273 from the Gene Expression Omnibus

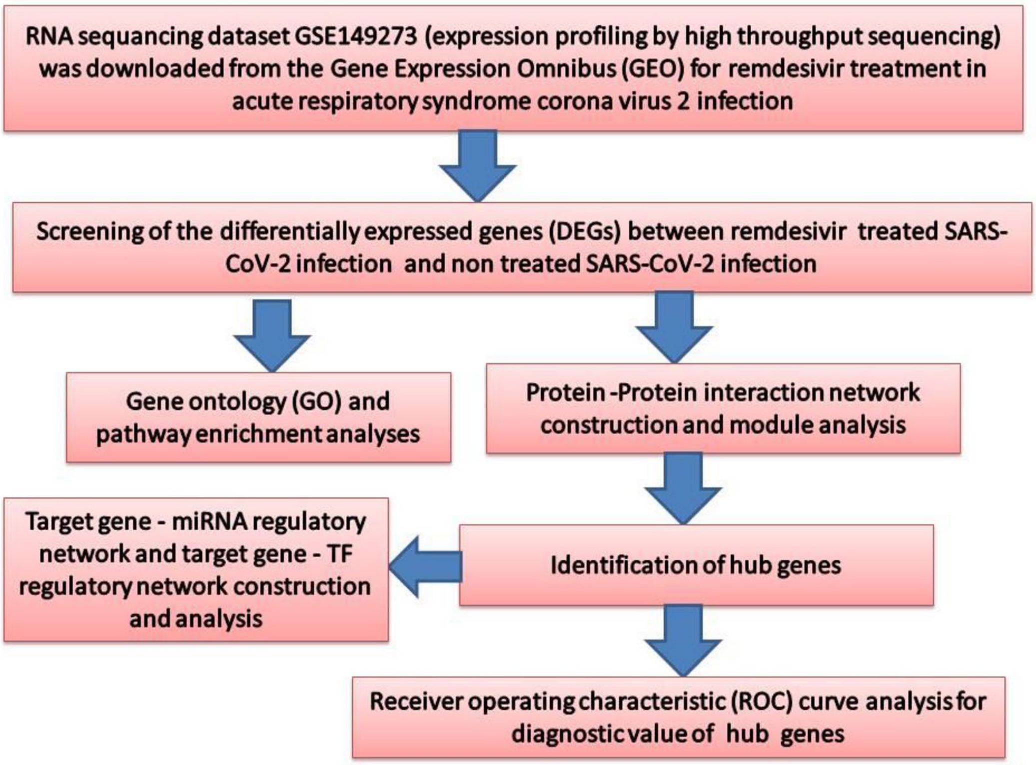

Figure 1. Flowchart of this study.

(GEO) database (http://www.ncbi.nlm.nih.gov/geo/)[6] and conducted a bioinformatics analysis to study the DEGs between remdesivir-treated SARS-CoV-2 infection samples and non-treated SARS-CoV-2 infection samples. We performed gene ontology (GO) and pathway enrichment analyses, protein-protein interaction (PPI) network construction and analysis, modules analysis, target gene—miRNA regulatory network, and target gene—TF regulatory network construction and analysis. Finally, we performed receiver-operating characteristic (ROC) analyses for diagnostic values of hub genes. The findings in our study may contribute to novel molecular changes during remdesivir treatment for SARS-CoV-2 infection.

Materials and Methods

Data resource

The study was designed according to the flowchart (Figure 1). Expression profiling by high-throughput sequencing dataset GSE149273 based on GPL21290 Illumina HiSeq 3000 (Homo sapiens) platform was downloaded from the GEO database, a public depository database of gene expression data. GSE149273 contains 60 samples, including 30 remdesivir-treated SARS-CoV-2 infection samples and 30 nontreated SARS-CoV-2 infection samples.

Screening of the DEGs

For the expression profiling by high-throughput sequencing dataset, the R package limma[7] was applied for performing the differential analysis between 30 remdesivir-treated SARS-CoV-2 infection samples and nontreated SARS-CoV-2 infection samples. The *P* values were adjusted by Benjamini and Hochberg method.[8] Based on the |log fold change (FC)| values and the *P* values, the DEGs (thresholds: $|logFC| > 1.3$ for upregulated genes and $|logFC| < -1.3$ for downregulated genes, adjusted $P < .05$).

Pathway enrichment analysis for DEGs

To analyze the functions of DEGs, BIOCYC (https://biocyc.org/),[9] Kyoto Encyclopedia of Genes and Genomes (http://www.genome.jp/kegg/pathway.html),[10] Pathway Interaction Database (https://wiki.nci.nih.gov/pages/viewpage.action?pageId=315491760),[11] REACTOME (https://reactome.org/),[12] GenMAPP (http://www.genmapp.org/),[13] MSigDB C2 BIOCARTA (http://software.broadinstitute.org/gsea/msigdb/collections.jsp),[14] PantherDB (http://www.pantherdb.org/),[15] Pathway Ontology (http://www.obofoundry.org/ontology/pw.html),[16] and Small Molecule Pathway Database (http://smpdb.ca/)[17] pathway analysis were performed by using the ToppGene (ToppFun) (https://toppgene.cchmc.org/enrichment.jsp)[18] online tool. $P < .05$ was set as the cut-off point.

Gene ontology enrichment analysis for DEGs

The ToppGene (ToppFun) (https://toppgene.cchmc.org/enrichment.jsp)[18] was used to study GO enrichment analyses of DEGs. The ToppGene online tool for GO analysis (http://

www.geneontology.org)[19] was used to complete the function of DEGs. Data from biological processes (BP), cellular components (CC), and molecular functions (MF) were documented from each set of genes. A $P < .05$ was considered statistically significant for all analyses.

Protein-protein interaction network construction and module analysis

The IMEX: The International Molecular Exchange Consortium (https://www.imexconsortium.org/)[20] is a biological database designed for predicting PPI networks and integrated with PPI databases such as Database of Interacting Proteins (http://dip.doe-mbi.ucla.edu/dip/Main.cgi),[21] IntAct Molecular Interaction Database (https://www.ebi.ac.uk/intact/),[22] the Molecular INTeraction database (https://mint.bio.uniroma2.it/),[23] InnateDB (https://www.innatedb.com/),[24] Human Protein Reference Database (http://www.hprd.org/),[25] BioGRID (https://thebiogrid.org/),[26] Integrated Interactions Database from a well-known online server (http://iid.ophid.utoronto.ca),[27] and MatrixDB (http://matrixdb.univ-lyon1.fr/).[28] Cytoscape (http://www.cytoscape.org/, version 3.8.0),[29] open software, was used to visualize the PPI networks. The top genes with the highest node degree,[30] betweenness centrality,[31] stress centrality,[32] closeness centrality,[31] and lowest clustering coefficient[33] were considered as hub genes based on the analysis using NetworkAnalyzer from Cytoscape. PEWCC1 (http://apps.cytoscape.org/apps/PEWCC1),[34] a plugin of Cytoscape, can screen a significant module from the PPI network.

Construction of target genes—miRNA regulatory network

The miRNet database (https://www.mirnet.ca/)[35] is the biggest collection of predicted and experimentally verified target gene—miRNA interactions using 10 algorithms such as TarBase (http://diana.imis.athena-innovation.gr/DianaTools/index.php?r=tarbase/index),[36] miRTarBase (http://mirtarbase.mbc.nctu.edu.tw/php/download.php),[37] miRecords (http://miRecords.umn.edu/miRecords),[38] miR2Disease (http://www.mir2disease.org/),[39] HMDD (http://www.cuilab.cn/hmdd),[40] PhenomiR (http://mips.helmholtz-muenchen.de/phenomir/),[41] SM2miR (http://bioinfo.hrbmu.edu.cn/SM2miR/),[42] PharmacomiR (http://www.pharmaco-mir.org/),[43] EpimiR (http://bioinfo.hrbmu.edu.cn/EpimiR/),[44] and starBase (http://starbase.sysu.edu.cn/).[45] Target genes—miRNA regulatory network among upregulated and downregulated genes was constructed by Cytoscape (http://cytoscape.org/).[29]

Construction of target genes—TF regulatory network

The NetworkAnalyst database (https://www.networkanalyst.ca/)[46] is the biggest collection of predicted and experimentally verified target gene—TF interactions using JASPAR (http://jaspar.genereg.net/)[47] database. Target genes—TF regulatory network among upregulated and downregulated genes was constructed by Cytoscape (http://cytoscape.org/).[29]

Validation of hub genes

To identify the diagnostic value of upregulated and downregulated hub genes in SARS-CoV-2 infection, pROC package[48] in R language to illustrate ROC curves was used in this investigation and area under the curve (AUC) of ROC curves was determined to check the act of each upregulated and downregulated hub genes. When the AUC value was greater than 0.6, the upregulated and downregulated hub genes were able of distinguishing remdesivir-treated SARS-CoV-2 infection samples and nontreated SARS-CoV-2 infection samples. The diagnostic value of upregulated and downregulated hub genes in GSE149273 dataset was estimated in our research work.

Results

Screening of the DEGs

A total of 909 DEGs (453 upregulated genes and 457 downregulated genes) were identified between remdesivir-treated SARS-CoV-2 infection and nontreated SARS-CoV-2 infection ($|\text{logFC}| > 1.3$ for upregulated genes and $|\text{logFC}| < -1.3$ for downregulated genes, adjusted $P < .05$) and volcano plots showing the results of differential analysis are given in Figure 2. The upregulated genes and downregulated genes are listed in Supplemental Table 1. Heatmaps are shown in Figures 3 and 4, respectively.

Pathway enrichment analysis for DEGs

To further understand the function and mechanism of the identified upregulated and downregulated genes, pathway enrichment analysis was performed using the ToppGene web tool. Upregulated genes were particularly enriched in pyrimidine deoxyribonucleoside degradation, tryptophan degradation to 2-amino-3-carboxymuconate semialdehyde, influenza A, cytokine-cytokine receptor interaction, IL23-mediated signaling events, direct p53 effectors, cytokine signaling in immune system, interferon signaling, C21 steroid hormone metabolism, purine metabolism, genes encoding secreted soluble factors, ensemble of genes encoding extracellular matrix (ECM)-associated proteins including ECM-affiliated proteins, ECM regulators and secreted factors, toll receptor signaling pathway, inflammation mediated by chemokine and cytokine signaling pathway, JAK-STAT signaling, purine metabolic, steroidogenesis, and pyrimidine metabolism are listed in Supplemental Table 2. Similarly, downregulated genes were notably enriched in pyridoxal 5′-phosphate salvage, glutamine degradation/glutamate biosynthesis, drug metabolism—cytochrome P450, chemical carcinogenesis, signaling events mediated by the hedgehog family, glypican 2 network,

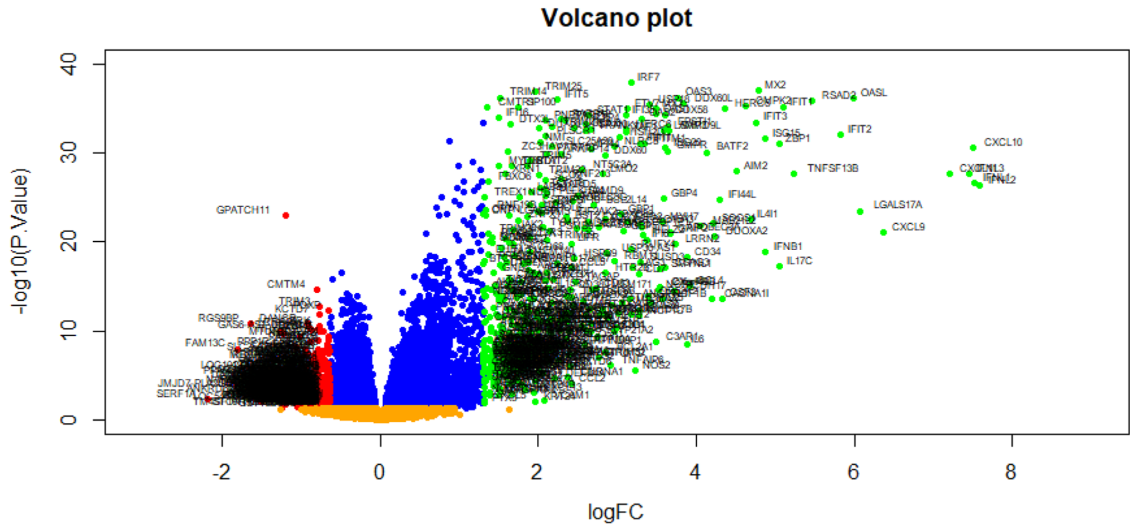

Figure 2. Volcano plot of differentially expressed genes. Genes with a significant change of more than 2-fold were selected. Green dot represented upregulated significant genes and red dot represented downregulated significant genes.

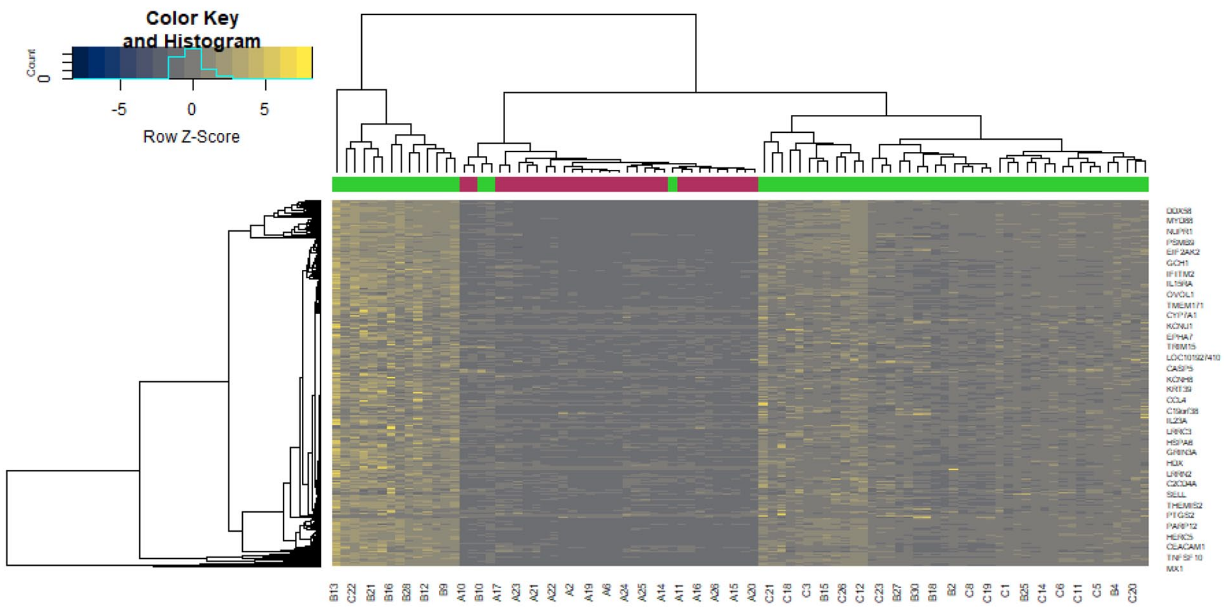

Figure 3. Heat map of upregulated differentially expressed genes. Legend on the top left indicates log fold change of genes (A1-A30 = nontreated SARS-CoV-2 infection samples [blue color box]; B1-B30 = remdesivir-treated SARS-CoV-2 infection samples [green color box]). SARS-CoV-2 indicates severe acute respiratory syndrome corona virus 2.

GPCR ligand binding, phase 2—plateau phase, glycolysis, gluconeogenesis, type III secretion system, genes encoding secreted soluble factors, ensemble of genes encoding ECM-associated proteins including ECM-affiliated proteins, ECM regulators and secreted factors, notch signaling pathway, transforming growth factor-beta signaling pathway, notch signaling, wnt signaling, sulfate/sulfite metabolism, and leukotriene C4 synthesis deficiency are listed in Supplemental Table 3.

Gene ontology enrichment analysis for DEGs

Gene ontology term enrichment analysis was performed using web tool ToppGene. Supplemental Tables 4 and 5 show the functions of the identified upregulated and downregulated genes. Upregulated genes of BP were associated with defense response and response to external biotic stimulus. Downregulated genes of BP were associated with reproductive process and positive regulation of transcription by RNA polymerase II. Upregulated genes of CC were associated with cell surface and external side of plasma membrane. Downregulated genes of CC were associated with intrinsic component of plasma membrane and nuclear chromatin. Upregulated genes of MF were associated with cytokine activity and receptor ligand activity. Downregulated genes of MF were associated with transporter activity and cation transmembrane transporter activity.

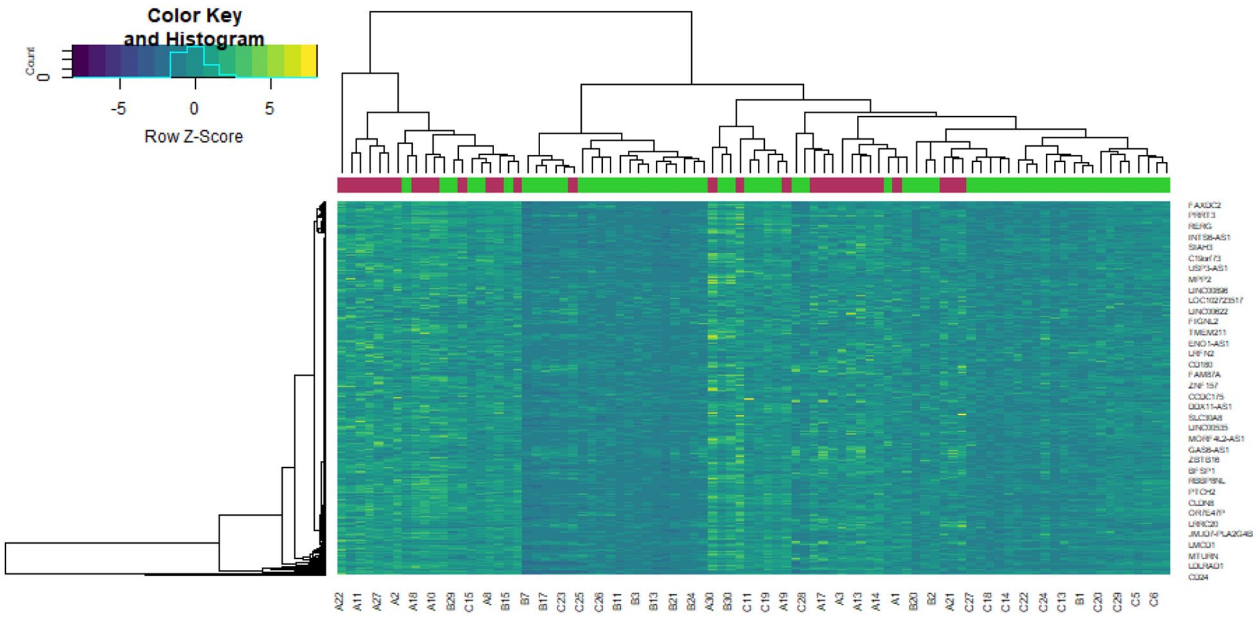

Figure 4. Heat map of downregulated differentially expressed genes. Legend on the top left indicates log fold change of genes (A1-A30 = nontreated SARS-CoV-2 infection samples [blue color box]; B1-B30 = remdesivir-treated SARS-CoV-2 infection samples [green color box]). SARS-CoV-2 indicates severe acute respiratory syndrome corona virus 2.

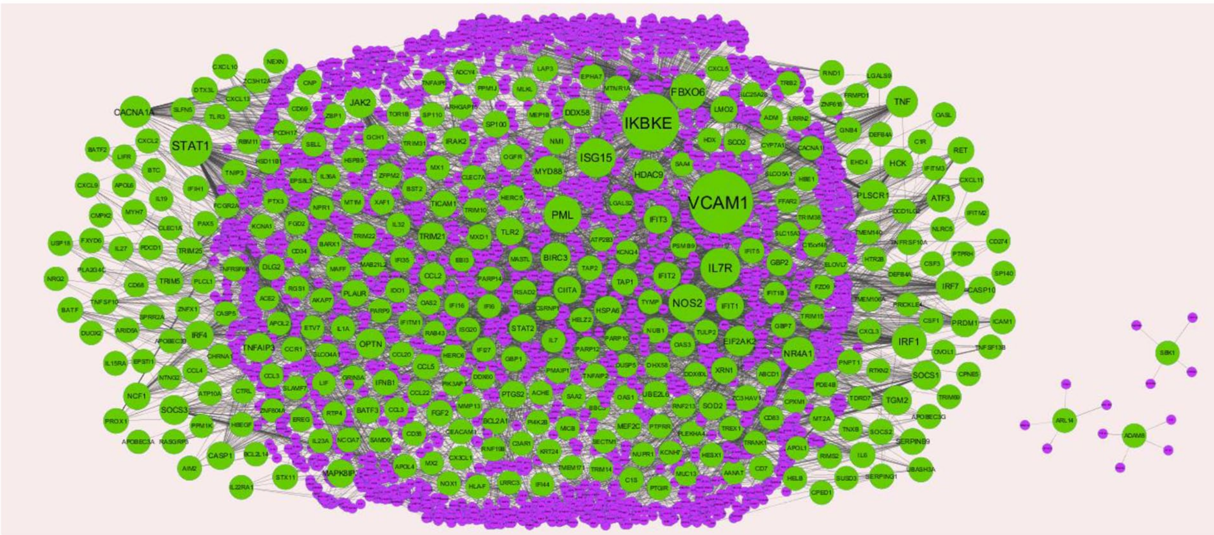

Figure 5. Protein-protein interaction network of upregulated genes. Green nodes denote upregulated genes.

Protein-protein interaction network construction and module analysis

The PPI network of upregulated genes consisting of 206 nodes and 412 edges was constructed in the IMEX database (Figure 5). Top hub genes were selected by the NetworkAnalyzer (Supplemental Table 6), including VCAM1, IKBKE, STAT1, IL7R, ISG15, PML, NOS2, FBXO6, IRF1, IRF7, ADAM8, SBK1, ARL14, and TGM2, and statistical results in scatter plot for node degree distribution, betweenness centrality, stress centrality, closeness centrality, and clustering coefficient are displayed in Figure 6A to E. Enrichment analysis revealed that hub genes in PPI network were mainly associated with malaria, influenza A, defense response, cytokine-cytokine receptor interaction, cytokine signaling in immune system, direct p53 effectors, activating transcription factor-2 transcription factor network, adaptive immune system, IL6-mediated signaling events, measles, innate immune system, and ensemble of genes encoding ECM-associated proteins including ECM-affiliated proteins, ECM regulators, and secreted factors. Similarly, PPI network of downregulated genes consisting of 206 nodes and 412 edges was constructed in the IMEX database (Figure 7). Top hub genes were selected by the NetworkAnalyzer (Supplemental Table 6), including E2F1, ZBTB16, TFAP4, ATP6V1B1, APBB1, ELF5, CBX2, USP2, ERP27, DSCAML1, KCNF1, DLX3, EGFL6, and AMIGO1, and statistical results in scatter plot for node degree distribution,

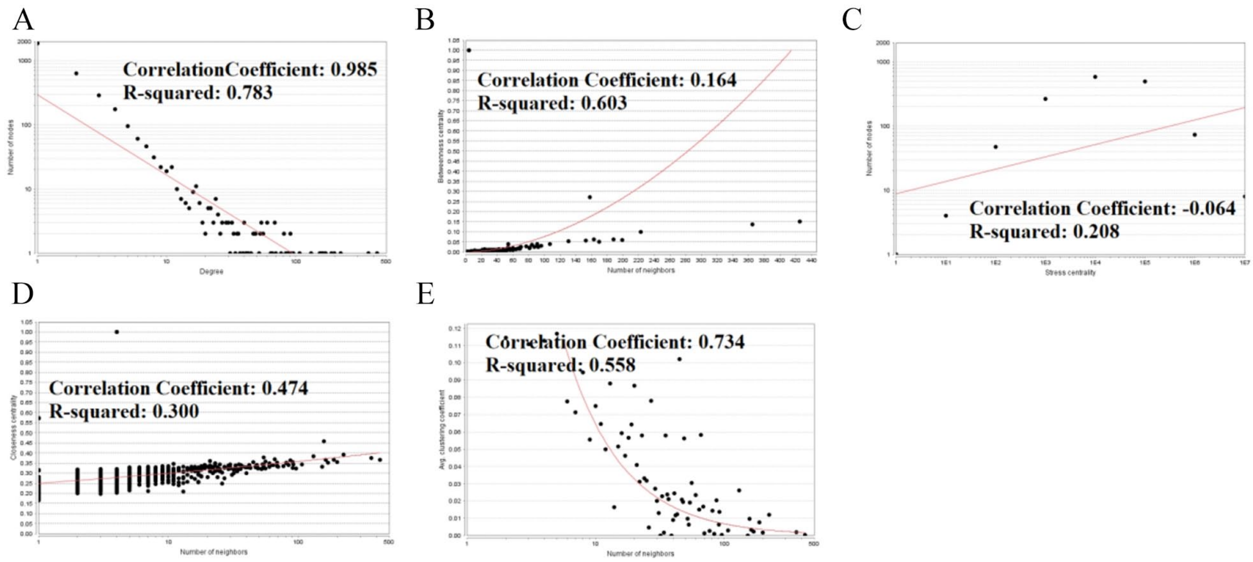

Figure 6. Scatter plot for upregulated genes. (A) Node degree. (B) Betweenness centrality. (C) Stress centrality. (D) Closeness centrality. (E) Clustering coefficient.

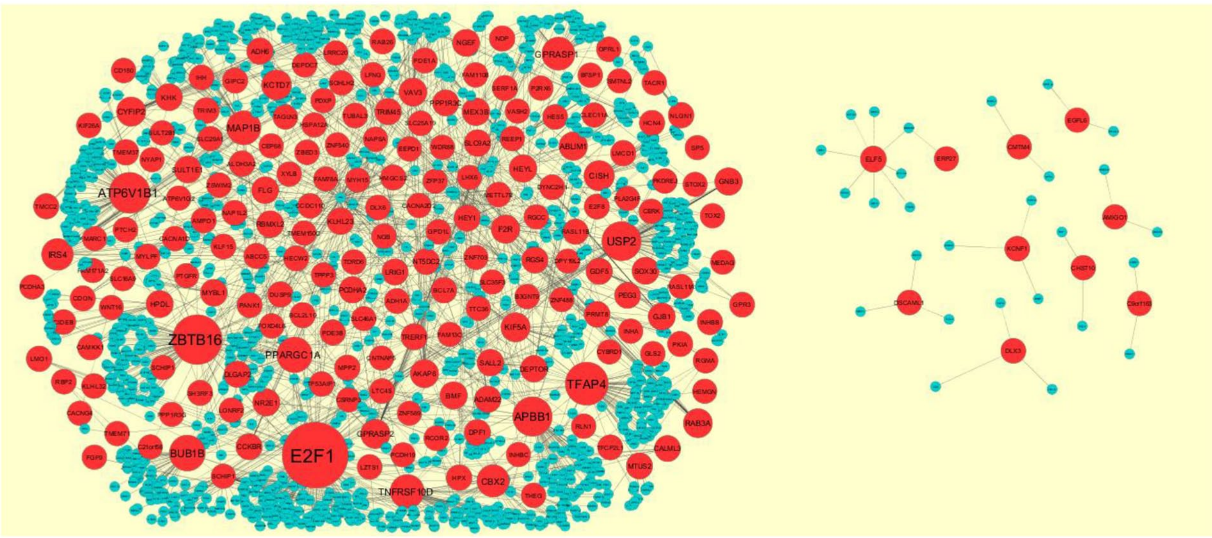

Figure 7. Protein-protein interaction network of downregulated genes. Red nodes denote downregulated genes.

betweenness centrality, stress centrality, closeness centrality, and clustering coefficient are displayed in Figure 8A to E. Enrichment analysis revealed that hub genes in PPI network were mainly associated with notch-mediated HES/HEY network, map kinase inactivation of SMRT corepressor, positive regulation of transcription by RNA polymerase II, iron uptake and transport, positive regulation of RNA metabolic process, nuclear chromatin, reproductive process, positive regulation of developmental process, de novo pyrimidine ribonucleotide biosynthesis, neuronal system, transcription regulatory region sequence-specific DNA binding, signaling receptor binding, and MF regulator.

Analysis using the PEWCC1 Cytoscape software plugin was used to create modules for the PPI networks. A total of 423 modules were created from PPI network of upregulated genes. Four significant modules were identified: module 1 (nodes 44 and edges 173), module 6 (nodes 24 and edges 69), module 12 (nodes 20 and edges 38), and module 16 (nodes 18 and edges 33) are shown in Figure 9. Enrichment analysis revealed that hub genes in modules were mainly associated with influenza A, measles, chemokine signaling pathway, cytokine signaling in immune system, defense response, response to external biotic stimulus, and innate immune response. A total of 219 modules were created from PPI network of downregulated genes. Four significant modules were identified: module 4 (nodes 87 and edges 86), module 5 (nodes 77 and edges 76), module 13 (nodes 41 and edges 41), and module 16 (nodes 29 and edges 28) are shown in Figure 10. Enrichment analysis revealed that hub genes in modules were mainly associated with multiorganism reproductive process, iron uptake and transport, neuroactive ligand-receptor interaction, and cell-cell signaling.

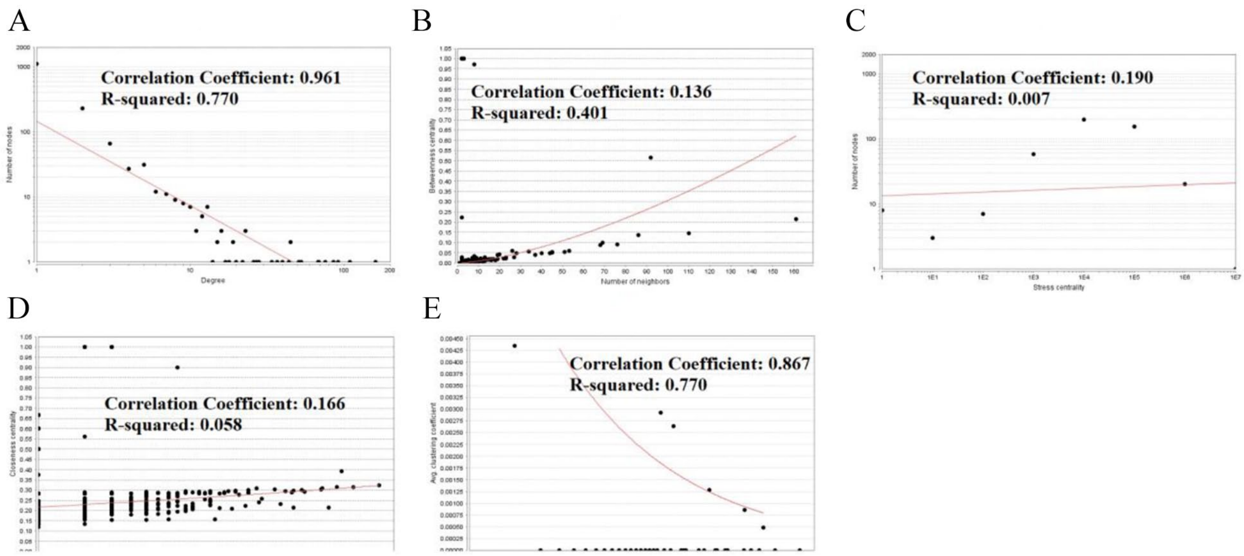

Figure 8. Scatter plot for downregulated genes. (A) Node degree. (B) Betweenness centrality. (C) Stress centrality. (D) Closeness centrality. (E) Clustering coefficient.

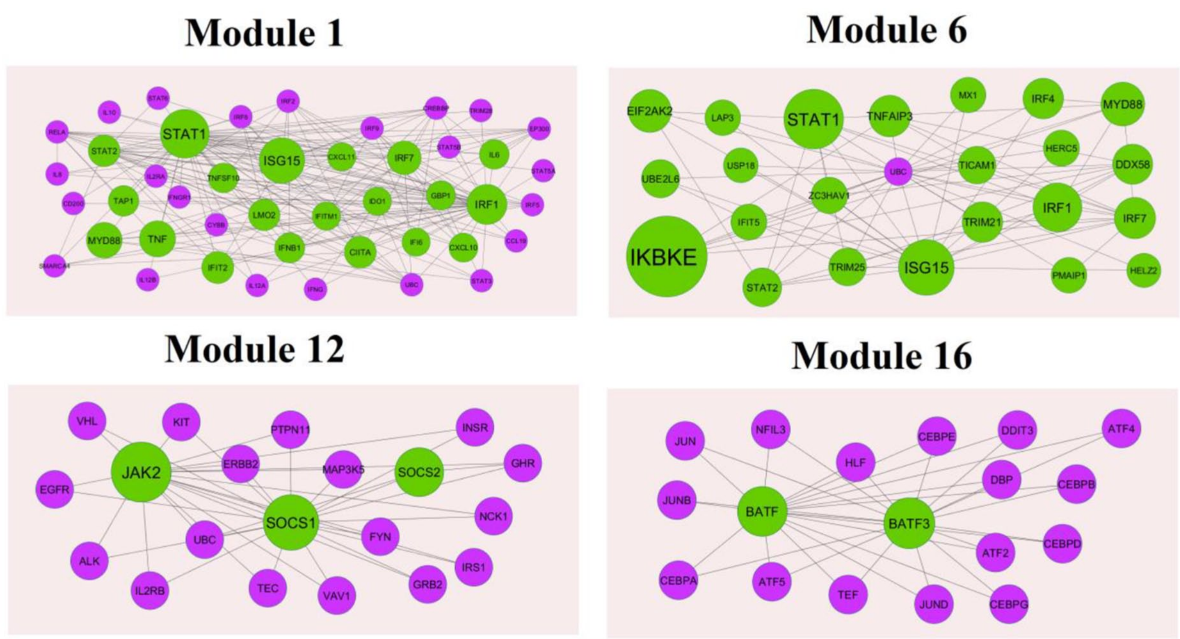

Figure 9. Modules in PPI network. The green nodes denote the upregulated genes. PPI indicates protein-protein interaction.

Construction of target genes—miRNA regulatory network

The upregulated and downregulated genes were analyzed using the miRNet database. Target genes—miRNA regulatory network for upregulated genes consisting of 2182 nodes (1862 miRNAs and 320 upregulated genes) and 5899 edges (Figure 11). The results of the topological property analysis demonstrated that SOD2 (degree = 257; ex, hsa-mir-4298), PMAIP1 (degree = 147; ex, hsa-mir-5697), APOL6 (degree = 127; ex, hsa-mir-4478), ICOSLG (degree = 119; ex, hsa-mir-4739), and NPR1 (degree = 118; ex, hsa-mir-6131) are listed in Supplemental Table 7. Enrichment analyses revealed that target genes in network were mainly associated with cytokine-mediated signaling pathway, viral carcinogenesis, adaptive immune system, and purine metabolism. Target genes—miRNA regulatory network for downregulated genes consisting of 2345 nodes (1783 miRNAs and 262 downregulated genes) and 4885 edges (Figure 12). The results of the topological property analysis demonstrated that VAV3 (degree = 165; ex, hsa-mir-4315), ZNF703 (degree = 115; ex, hsa-mir-5787), FAXC (degree = 112; ex, hsa-mir-4279), GPR137C (degree = 97; ex, hsa-mir-3914), and ZNF704 (degree = 86; ex, hsa-mir-1538) are listed in Supplemental Table 7. Enrichment analysis revealed that target genes in network were mainly associated with regulation of actin cytoskeleton, positive regulation of developmental process, and transcription regulatory region sequence-specific DNA binding.

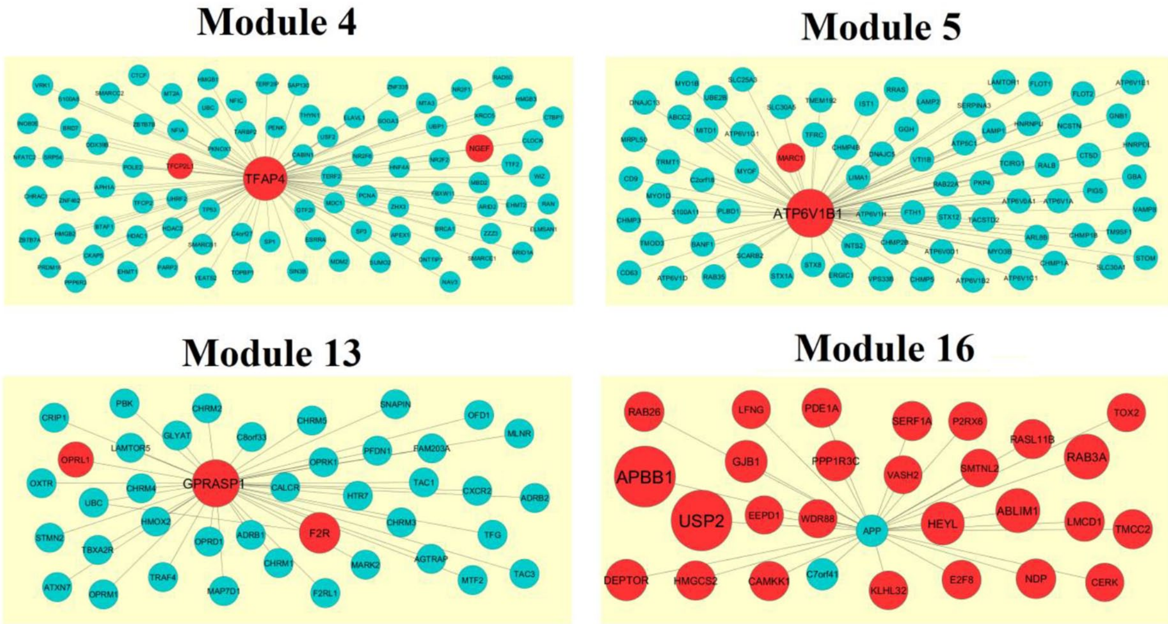

Figure 10. Modules in PPI network. The red nodes denote the downregulated genes. PPI indicates protein-protein interaction.

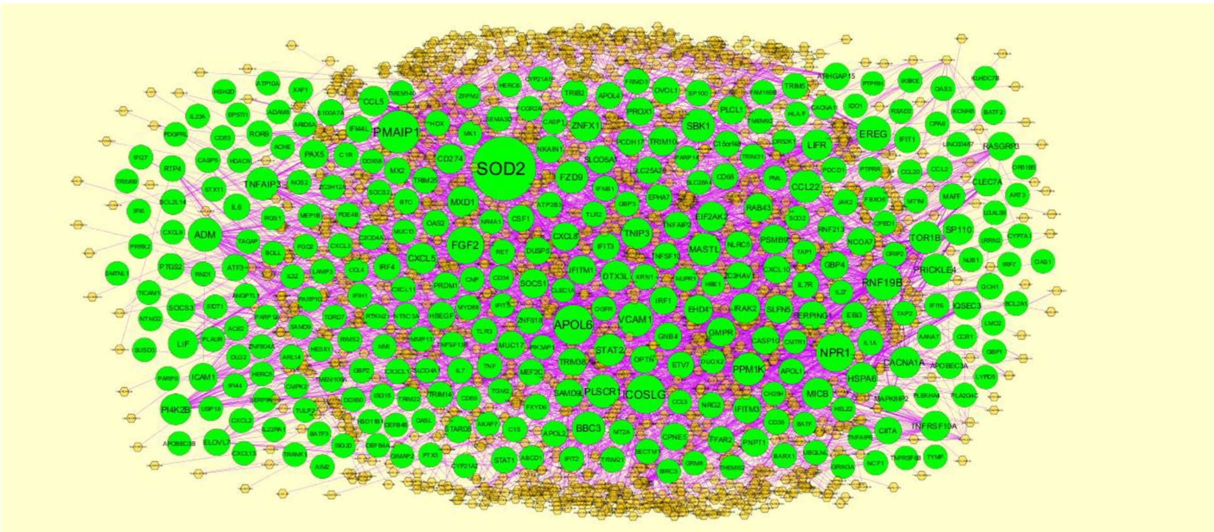

Figure 11. The network of upregulated genes and their related miRNAs. The green circle nodes are the upregulated genes, and yellow diamond nodes are the miRNAs.

Construction of target genes—TF regulatory network

The upregulated and downregulated genes were analyzed using the NetworkAnalyst database. Target genes—TF regulatory network for upregulated genes consisting of 516 nodes (92 TFs and 424 upregulated genes) and 3459 edges (Figure 13). The results of the topological property analysis demonstrated that CD7 (degree = 265; ex, FOXC1), ELOVL7 (degree = 195; ex, GATA2), NTNG2 (degree = 136; ex, YY1), CXCL2 (degree = 125; ex, FOXL1), and (degree = 102; ex, NFKB1) are listed in Supplemental Table 8. Enrichment analysis revealed that target genes in network were mainly associated with fas signaling pathway, ensemble of genes encoding ECM and ECM-associated proteins, ensemble of genes encoding ECM and ECM-associated proteins, and influenza A. Target genes—TF regulatory network for downregulated genes consisting of 516 nodes (80 TFs and 458 downregulated genes) and 2424 edges (Figure 14). The results of the topological property analysis demonstrated that ABCA17P (degree = 217; ex, FOXC1), TACR1 (degree = 182; ex, GATA2), REEP1 (degree = 97; ex, YY1), TRAM1L1 (degree = 97; ex, FOXL1), and FGF9 (degree = 74; ex, TFAP2A) are listed in Supplemental Table 8. Enrichment analysis revealed that target genes in network were mainly associated with calcium signaling pathway, signaling receptor binding, transmembrane transport, and cell-cell signaling.

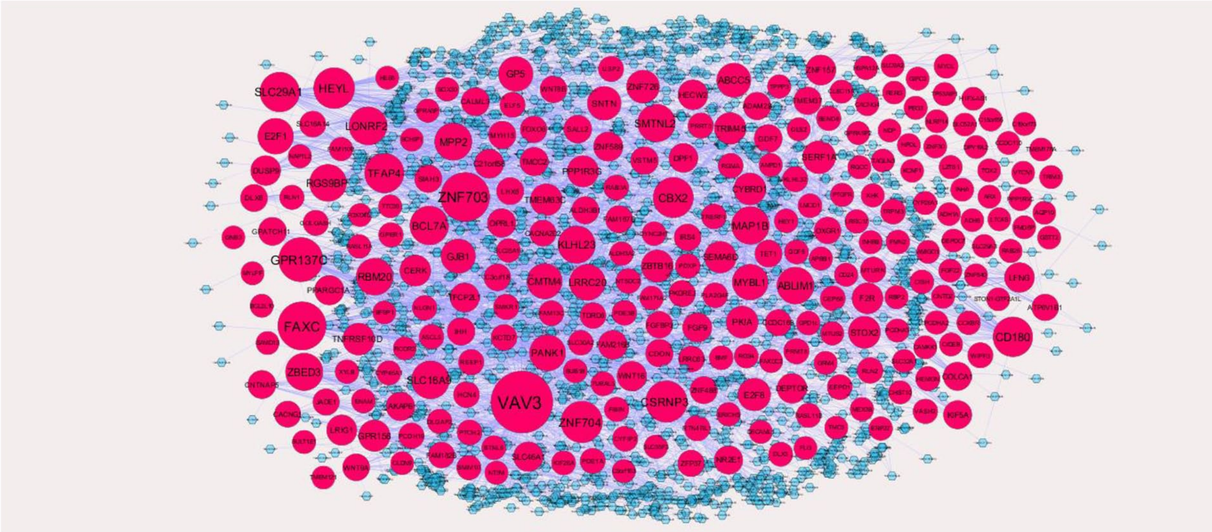

Figure 12. The network of downregulated genes and their related miRNAs. The red circle nodes are the downregulated genes, and blue diamond nodes are the miRNAs.

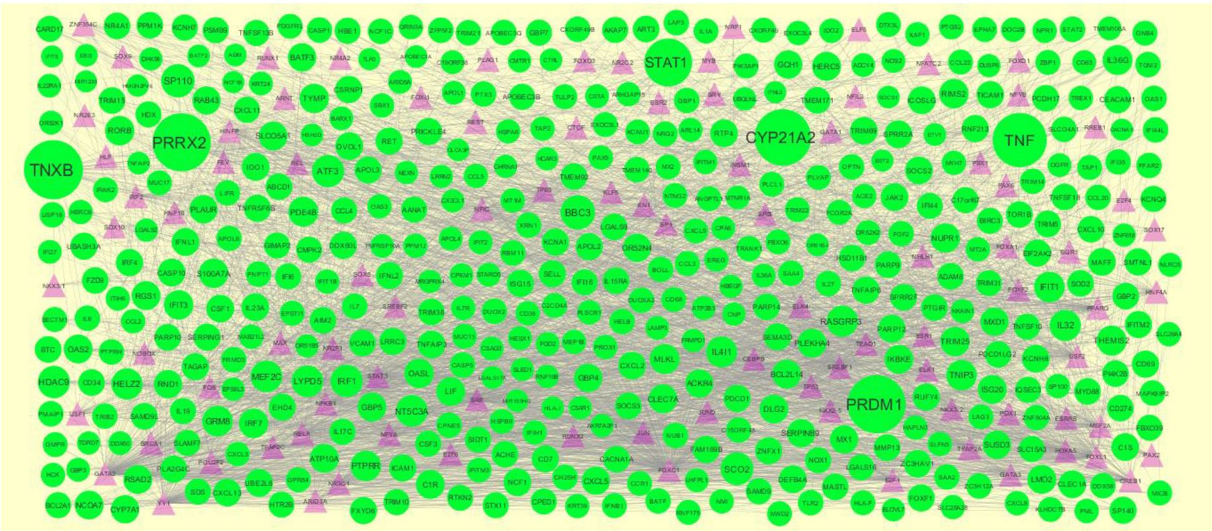

Figure 13. The network of upregulated genes and their related TFs. The green circle nodes are the upregulated genes, and purple triangle nodes are the TFs.

Validation of hub gene

The prediction achievement by ROC analysis showed that as single classifiers, CIITA, HSPA6, MYD88, SOCS3, TNFRSF10A, ADH1A, CACNA2D2, DUSP9, FMO5, and PDE1A had significant predictive values with AUCs of 0.956, 0.752, 0.992, 0.914, 0.837, 0.759, 0.781, 0.788, 0.833, and 0.788, and *P* values of .00022, .00714, .00152, .00038, .00054, .00275, .00093, .00092, .00294, and .00252, respectively (Figure 15).

Discussion

Outbreaks of appearing and reappearing of SARS-CoV-2 infection are frequent threats to human health across globe. When a novel virus was detected and linked with human disease, it is necessary to understand molecular changes during antiviral treatment in SARS-CoV-2 infection.[49] In this investigation, we performed a series of bioinformatics analysis to screen hub genes and pathways were associated with remdesivir-treated SARS-CoV-2 infection. The expression profiling by high-throughput RNA sequencing found that 49 upregulated genes and 72 downregulated genes were identified in remdesivir-treated SARS-CoV-2 infection compared with nontreated SARS-CoV-2 infection. IRF7,[50] MX2,[51] TRIM25,[52] TRIM14,[53] IFIT5,[54] and IFIT1[55] have been shown to be a meaningful advance factor for progression of influenza virus infection, but these novel genes expressed in remdesivir-treated SARS-CoV-2 infection. Genes including OAS3,[56] OASL (2′-5′-oligoadenylate synthetase like),[57] and USP18[58] were a preferred anticancer target, but these novel genes expressed in remdesivir-treated SARS-CoV-2 infection. Kurokawa et al[59]

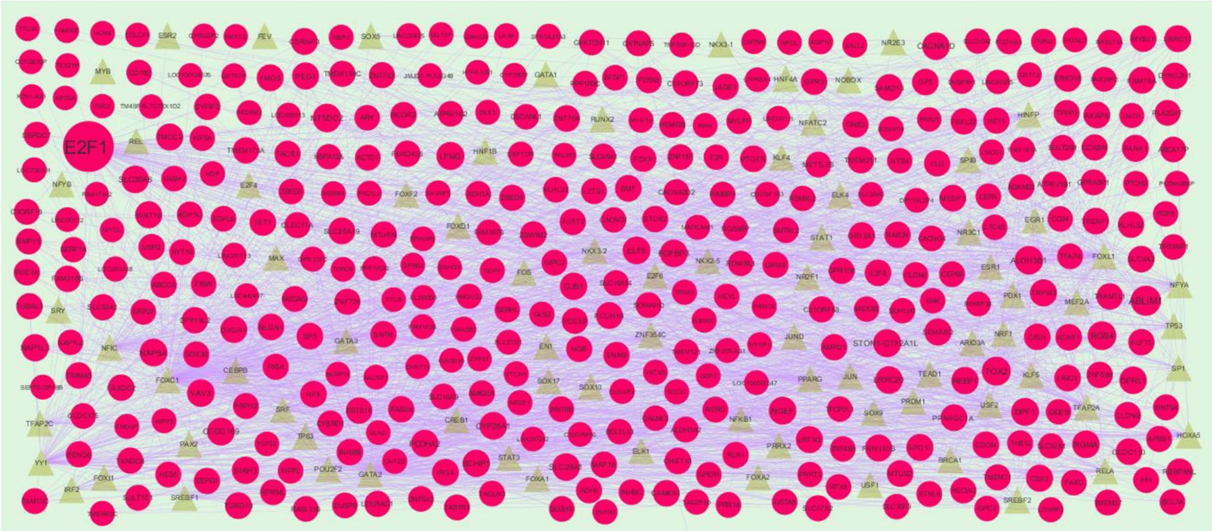

Figure 14. The network of downregulated genes and their related TFs. The green circle nodes are the downregulated genes, and blue triangle nodes are the TFs.

demonstrated that altered expression of RSAD2 during measles virus infection, but this novel gene might be expressed in remdesivir-treated SARS-CoV-2 infection.

The ToppGene online tool was used to perform a pathway enrichment analysis. Xia et al[60] showed that DDX58 promoted aggressiveness of measles virus infection, but this novel gene was expressed in remdesivir-treated SARS-CoV-2 infection. CIITA (class II major histocompatibility complex transactivator),[61] CCL2,[62] PML (promyelocytic leukemia),[63] ICAM1,[64] IL1A,[65] MX1,[66] CXCL8,[67] MYD88,[67] CXCL10,[68] STAT1,[69] STAT2,[70] SOCS3,[71] CASP1,[72] TLR3,[73] TNF (tumor necrosis factor),[74] IL32,[75] TRIM22,[76] IFITM3,[77] FGF2,[78] IFITM1,[79] IFITM2,[80] IFI27,[81] ISG15,[82] SOCS1,[83] IRF1,[84] ISG20,[85] IL22RA1,[86] SOCS2,[87] GBP5,[88] BST2,[89] HERC5,[90] IL27,[91] CXCL13,[92] CXCL3,[93] TLR2,[94] and TNFAIP3[95] proved to be positively correlated with the progress of influenza virus infection, but these novel genes were expressed in remdesivir-treated SARS-CoV-2 infection. CCL5,[96] IL19,[97] CCL3,[96] CCL4,[98] CCL20,[99] IFIT3,[100] CSF3,[101] and IL7R[102] proved to be an independent diagnostic factors in respiratory syncytial virus infection, but these novel genes were expressed in remdesivir-treated SARS-CoV-2 infection. Conti et al[103] and Wu and Yang[104] found expression of IL6 and JAK2 was correlated with SARS-CoV-2 infection progression. TICAM1,[105] OAS1,[106] OAS2,[107] CXCL9,[108] EREG (epiregulin),[109] CCL22,[110] VCAM1,[111] IFI35,[112] IFIT2,[113] TRIM5,[114] XAF1,[115] IFI6,[116] IL7,[117] SP100,[118] GBP1,[119] GBP2,[120] IRF4,[121] MIR5193,[122] IFNL3,[123] CYP21A2,[124] CXCL5,[125] CX3CL1,[126] CCL4L1,[127] WNT16,[128] GNB3,[129] FLG (filaggrin),[130] and HEY1[131] have been found to be differentially expressed in various viral infections, but these novel genes were expressed in remdesivir-treated SARS-CoV-2 infection. Sanders et al[132] believed that NOS2 plays an important role in the pathophysiology of rhinovirus infection, but this novel gene was expressed in remdesivir-treated SARS-CoV-2 infection. Bonville et al[133] reported that the expression of the gene CCR1 is correlated with pneumovirus infection, but this novel gene was expressed in remdesivir-treated SARS-CoV-2 infection. IRAK2 is a promising biomarker in bronchitis virus infection[134] detection and diagnosis, but this novel gene was expressed in remdesivir-treated SARS-CoV-2 infection.

The functions of the upregulated and downregulated genes were identified by GO enrichment analysis. The involvement of TREX1,[135] IFNL4,[136] MICB (MHC class I polypeptide-related sequence B),[137] RAB43,[138] APOL1,[139] IFI16,[140] APOBEC3B,[141] SLAMF7,[142] HDAC9,[143] APOBEC3A,[144] SERPING1,[145] TAP2,[146] LAG3,[147] OPTN (optineurin),[148] CD68,[149] SP140,[150] PDCD1,[151] PLVAP (plasmalemma vesicle-associated protein),[152] CD34,[153] CD38,[154] CD69,[155] SLC30A8,[156] and ATP6V1G2[157] with various viral infections was demonstrated previously, but these novel genes were expressed in remdesivir-treated SARS-CoV-2 infection. The altered expression of APOBEC3G,[158] ADAM8,[159] ZBP1,[160] NLRC5,[161] AIM2,[162] DUOX2,[163] NOX1,[164] IDO1,[165] CEACAM1,[166] PTX3,[167] TAP1,[168] FFAR2,[169] and E2F1[170] was observed to be associated with the progression of influenza virus infection, but these novel genes were expressed in remdesivir-treated SARS-CoV-2 infection. Currently, CD83 has been reported to be very important in progression of respiratory syndrome virus infection,[171] but this novel gene was expressed in remdesivir-treated SARS-CoV-2 infection. ACE2 is recognized as an important molecular marker of SARS-CoV-2 infection.[172] Cheng et al[173] found the expression of NMI (N-myc and STAT interactor) in patients with severe acute respiratory syndrome corona virus infection, but this novel gene was expressed in remdesivir-treated SARS-CoV-2 infection. Previous studies had shown that the altered expression of CD274 was closely related to the occurrence of rhino virus

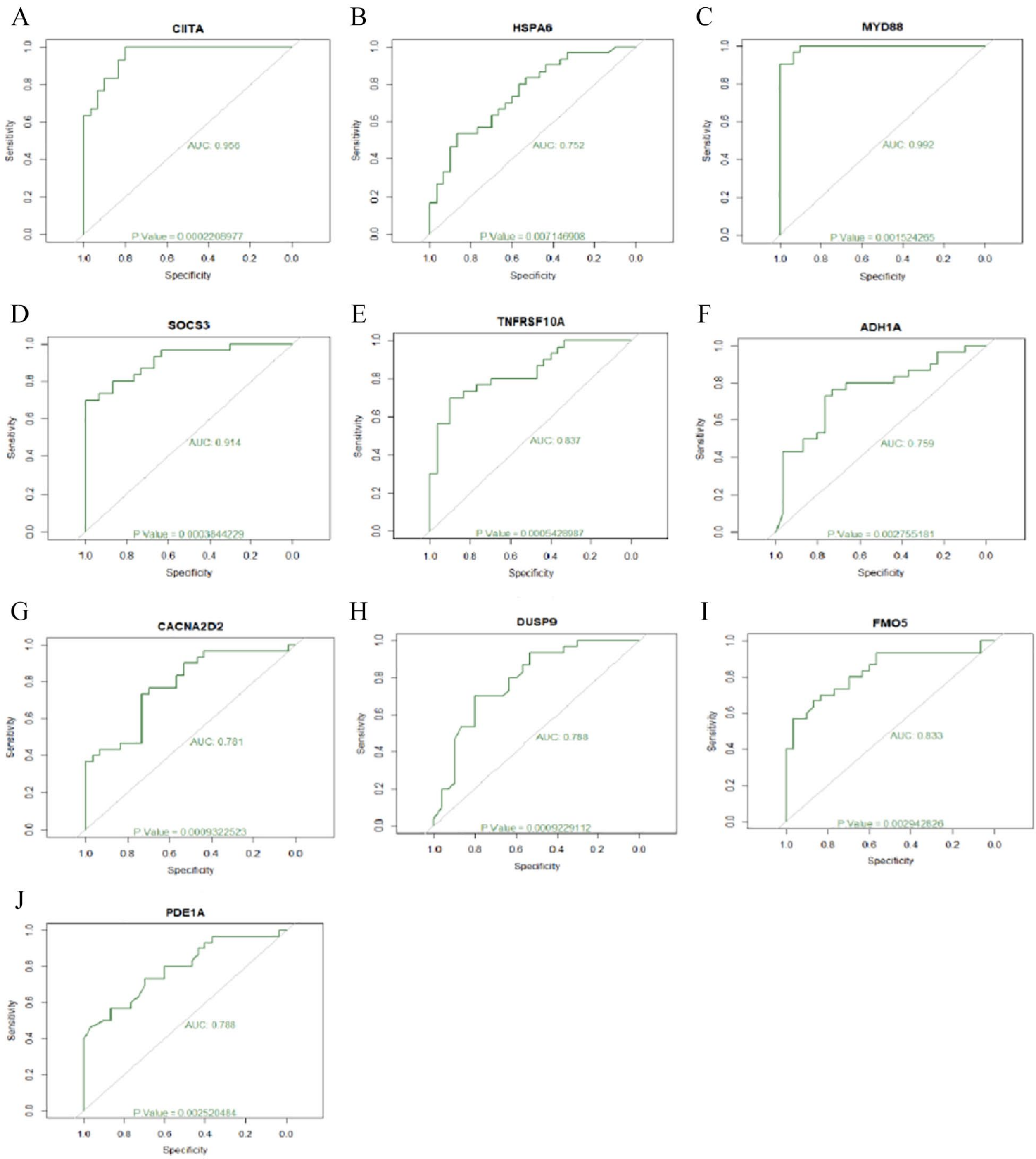

Figure 15. ROC curve validated the sensitivity and specificity of hub genes as a predictive biomarker for SARS-CoV-2 infection. (A) CIITA. (B) HSPA6. (C) MYD88. (D) SOCS3. (E) TNFRSF10A. (F) ADH1A. (G) CACNA2D2. (H) DUSP9. (I) FMO5. (J) PDE1A. ROC indicates receiver-operating characteristic; SARS-CoV-2, severe acute respiratory syndrome corona virus 2.

infection,[174] but this novel gene was expressed in remdesivir-treated SARS-CoV-2 infection.

The construction of protein-protein interaction network and module analysis for upregulated and downregulated genes have been proven to be useful in the analysis of hub genes involved in remdesivir-treated SARS-CoV-2 infection. Fusco et al[175] revealed that HELZ2 may be the potential targets for dengue virus infection diagnosis and treatment, but this novel gene was expressed in remdesivir-treated SARS-CoV-2 infection. BATF3 levels are correlated with disease severity in patients with respiratory poxvirus infection,[176] but this novel gene was expressed in remdesivir-treated SARS-CoV-2 infection. In general, our findings suggested that novel biomarkers such as FBXO6, SBK1, ARL14, LMO2, LAP3, TFAP4, APBB1, ELF5, USP2, ERP27, DSCAML1, NGEF (neuronal guanine nucleotide exchange factor), MARC1, GPRASP1, RAB26, DEPTOR (DEP domain containing MTOR interacting protein), HMGCS2, EEPD1, CAMKK1, PDE1A,

PPP1R3C, WDR88, SERF1A, KLHL32, SMTNL2, RASL11B, ABLIM1, TOX2, LMCD1, TMCC2, and CERK (ceramide kinase) might play key roles in the action mechanism of SARS-CoV-2 infection.

The construction of target genes—miRNA regulatory network—and target genes—TF regulatory network analysis for upregulated and downregulated genes—has been proven to be useful in the analysis of target genes involved in remdesivir-treated SARS-CoV-2 infection. Uckun et al[177] and Purdy et al[178] revealed that CD7 and ELOVL7 are associated with HIV infection, but these novel genes were expressed in remdesivir-treated SARS-CoV-2 infection. In general, our findings suggested that novel biomarkers such as SOD2, APOL6, NPR1, NTNG2, VAV3, ZNF703, FAXC (failed axon connections homolog, metaxin-like GST domain), GPR137C, ZNF704, ABCA17P, REEP1, and TRAM1L1 might play key roles in the action mechanism of remdesivir treated SARS-CoV-2 infection.

However, in addition to the objection of sample collection, huge obstacles in the analysis need to be overcome. In addition, due to the smallness of available datasets in the GEO database, the sample size in this study was finite. We will raise the sample size in a future investigation if Supplemental datasets can be replaced from the database.

In conclusion, we conducted a comprehensive bioinformatics analysis on NGS data of remdesivir-treated SARS-CoV-2 infection. Pivotal DEGs (upregulated and downregulated genes) and pathways were diagnosed and screened to provide a theoretical basis for molecular changes during antiviral treatment in SARS-CoV-2 infection. Ten hub genes, especially CIITA, HSPA6, MYD88, SOCS3, TNFRSF10A, ADH1A, CACNA2D2, DUSP9, FMO5, and PDE1A, were found to differentiate remdesivir-treated SARS-CoV-2 infection from nontreated SARS-CoV-2 infection. Nevertheless, additional relevant investigations are needed to further confirm the identified upregulated and downregulated genes, and pathways in remdesivir-treated SARS-CoV-2 infection.

Acknowledgements

We thank Eugene H Chang, The University of Arizona, Department of Otolaryngology, Eugene Lab, Tucson, Arizona, USA, very much, the author who deposited their next-generation sequencing dataset, GSE149273, into the public Gene Expression Omnibus database.

Author Contributions

GP helped in methodology and validation; BV helped in writing original draft, and review and editing; CV helped in software and investigation; and SK helped in supervision and validation.

Availability of Data and Materials

The datasets supporting the conclusions of this article are available in the Gene Expression Omnibus (https://www.ncbi.nlm.nih.gov/geo/) repository. ([GSE149273] https://www.ncbi.nlm.nih.gov/geo/query/acc.cgi?acc=GSE149273)

Ethical Approval

This article does not contain any studies with human participants or animals performed by any of the authors.

Informed Consent

No informed consent was obtained because this study does not contain human or animals participants.

ORCID iDs

Basavaraj Vastrad https://orcid.org/0000-0003-2202-7637
Chanabasayya Vastrad https://orcid.org/0000-0003-3615-4450

Supplemental Material

Supplemental material for this article is available online.

REFERENCES

1. Alhazzani W, Møller MH, Arabi YM, et al. Surviving Sepsis Campaign: guidelines on the management of critically ill adults with Coronavirus Disease 2019 (COVID-19). *Intensive Care Med*. 2020;46:854-887.
2. Ferner RE, Aronson JK. Remdesivir in covid-19. *BMJ*. 2020;369:m1610.
3. Elsawah HK, Elsokary MA, Abdallah MS, ElShafie AH. Efficacy and safety of remdesivir in hospitalized Covid-19 patients: systematic review and meta-analysis including network meta-analysis. *Rev Med Virol*. 2021;31:e2187.
4. Steuerman Y, Cohen M, Peshes-Yaloz N, et al. Dissection of influenza infection in vivo by single-cell RNA sequencing. *Cell Syst*. 2018;6:679-691e4.
5. Souza GAP, Salvador EA, de Oliveira FR, Cotta Malaquias LC, Abrahão JS, Leomil Coelho LF. An in silico integrative protocol for identifying key genes and pathways useful to understand emerging virus disease pathogenesis. *Virus Res*. 2020;284:197986.
6. Barrett T, Wilhite SE, Ledoux P, et al. NCBI GEO: archive for functional genomics data sets —update. *Nucleic Acids Res*. 2013;41:D991-D995.
7. Ritchie ME, Phipson B, Wu DI, et al. limma powers differential expression analyses for RNA-sequencing and microarray studies. *Nucleic Acids Res*. 2015;43:e47.
8. Abbas A, Kong XB, Liu Z, Jing BY, Gao X. Automatic peak selection by a Benjamini-Hochberg-based algorithm. *PLoS ONE*. 2013;8:e53112.
9. Caspi R, Billington R, Ferrer L, et al. The MetaCyc database of metabolic pathways and enzymes and the BioCyc collection of pathway/genome databases. *Nucleic Acids Res*. 2016;44:D471-D480.
10. Kanehisa M, Sato Y, Furumichi M, Morishima K, Tanabe M. New approach for understanding genome variations in KEGG. *Nucleic Acids Res*. 2019;47:D590-D595.
11. Schaefer CF, Anthony K, Krupa S, et al. PID: the Pathway Interaction Database. *Nucleic Acids Res*. 2009;37:D674-D679.
12. Fabregat A, Jupe S, Matthews L, et al. The Reactome Pathway Knowledgebase. *Nucleic Acids Res*. 2018;46:D649-D655.
13. Dahlquist KD, Salomonis N, Vranizan K, Lawlor SC, Conklin BR. GenMAPP, a new tool for viewing and analyzing microarray data on biological pathways. *Nat Genet*. 2002;31:19-20.
14. Subramanian A, Tamayo P, Mootha VK, et al. Gene set enrichment analysis: a knowledge-based approach for interpreting genome-wide expression profiles. *Proc Natl Acad Sci U S A*. 2005;102:15545-15550.
15. Mi H, Huang X, Muruganujan A, et al. PANTHER version 11: expanded annotation data from Gene Ontology and Reactome pathways, and data analysis tool enhancements. *Nucleic Acids Res*. 2017;45:D183-D189.
16. Petri V, Jayaraman P, Tutaj M, et al. The pathway ontology—updates and applications. *J Biomed Semantics*. 2014;5:7.
17. Jewison T, Su Y, Disfany FM, et al. SMPDB 2.0: big improvements to the Small Molecule Pathway Database. *Nucleic Acids Res*. 2014;42:D478-D484.
18. Chen J, Bardes EE, Aronow BJ, Jegga AG. ToppGene Suite for gene list enrichment analysis and candidate gene prioritization. *Nucleic Acids Res*. 2009;37:W305-W311.
19. Lewis SE. The vision and challenges of the gene ontology. *Methods Mol Biol*. 2017;1446:291-302.

20. Orchard S, Kerrien S, Abbani S, et al. Protein interaction data curation: the International Molecular Exchange (IMEx) consortium. *Nat Methods*. 2012;9:345-350.
21. Salwinski L, Miller CS, Smith AJ, Pettit FK, Bowie JU, Eisenberg D. The Database of Interacting Proteins: 2004 update. *Nucleic Acids Res*. 2004;32:D449-D451.
22. Orchard S, Ammari M, Aranda B, et al. The MIntAct project—IntAct as a common curation platform for 11—molecular interaction databases. *Nucleic Acids Res*. 2014;42:D358-D363.
23. Licata L, Briganti L, Peluso D, et al. MINT, the molecular interaction database: 2012 update. *Nucleic Acids Res*. 2012;40:D857-D861.
24. Breuer K, Foroushani AK, Laird MR, et al. InnateDB: systems biology of innate immunity and beyond—recent updates and continuing curation. *Nucleic Acids Res*. 2013;41:D1228-D1233.
25. Keshava Prasad TS, Goel R, Kandasamy K, et al. Human Protein Reference Database - 2009 update. *Nucleic Acids Res*. 2009;37:D767-D772.
26. Oughtred R, Stark C, Breitkreutz BJ, et al. The BioGRID interaction database: 2019 update. *Nucleic Acids Res*. 2019;47:D529-D541.
27. Kotlyar M, Pastrello C, Malik Z, Jurisica I. IID 2018 update: context-specific physical protein-protein interactions in human, model organisms and domesticated species. *Nucleic Acids Res*. 2019;47:D581-D589.
28. Clerc O, Deniaud M, Vallet SD, et al. MatrixDB: integration of new data with a focus on glycosaminoglycan interactions. *Nucleic Acids Res*. 2019;47:D376-D381.
29. Shannon P, Markiel A, Ozier O, et al. Cytoscape: a software environment for integrated models of biomolecular interaction networks. *Genome Res*. 2003;13:2498-2504.
30. Przulj N, Wigle DA, Jurisica I. Functional topology in a network of protein interactions. *Bioinformatics*. 2004;20:340-348.
31. Nguyen TP, Liu WC, Jordán F. Inferring pleiotropy by network analysis: linked diseases in the human PPI network. *BMC Syst Biol*. 2011;5:179.
32. Shi Z, Zhang B. Fast network centrality analysis using GPUs. *BMC Bioinformatics*. 2011;12:149.
33. Wang J, Li M, Wang H, Pan Y. Identification of essential proteins based on edge clustering coefficient. *IEEE/ACM Trans Comput Biol Bioinform*. 2012;9:1070-1080.
34. Zaki N, Efimov D, Berengueres J. Protein complex detection using interaction reliability assessment and weighted clustering coefficient. *BMC Bioinformatics*. 2013;14:163.
35. Fan Y, Xia J. miRNet-Functional analysis and visual exploration of miRNA-Target interactions in a network context. *Methods Mol Biol*. 2018;1819:215-233.
36. Vlachos IS, Paraskevopoulou MD, Karagkouni D, et al. DIANA-TarBase v7.0: indexing more than half a million experimentally supported miRNA:mRNA interactions. *Nucleic Acids Res*. 2015;43:D153-D159.
37. Chou CH, Shrestha S, Yang CD, et al. 2018: a resource for experimentally validated microRNA-target interactions. *Nucleic Acids Res*. 2018;46:D296-D302.
38. Xiao F, Zuo Z, Cai G, Kang S, Gao X, Li T. miRecords: an integrated resource for microRNA-target interactions. *Nucleic Acids Res*. 2009;37:D105-D110.
39. Jiang Q, Wang Y, Hao Y, et al. miR2Disease: a manually curated database for microRNA deregulation in human disease. *Nucleic Acids Res*. 2009;37:D98-D104.
40. Huang Z, Shi J, Gao Y, et al. HMDD v3.0: a database for experimentally supported human microRNA-disease associations. *Nucleic Acids Res*. 2019;47:D1013-D1017.
41. Ruepp A, Kowarsch A, Schmidl D, et al. PhenomiR: a knowledgebase for microRNA expression in diseases and biological processes. *Genome Biol*. 2010;11:R6.
42. Liu X, Wang S, Meng F, et al. SM2miR: a database of the experimentally validated small molecules' effects on microRNA expression. *Bioinformatics*. 2013;29:409-411.
43. Rukov JL, Wilentzik R, Jaffe I, Vinther J, Shomron N. Pharmaco-miR: linking microRNAs and drug effects. *Brief Bioinform*. 2014;15:648-659.
44. Dai E, Yu X, Zhang Y, et al. EpimiR: a database of curated mutual regulation between miRNAs and epigenetic modifications. *Database (Oxford)*. 2014;2014:bau023.
45. Li JH, Liu S, Zhou H, Qu LH, Yang JH. starBase v2.0: decoding miRNA-ceRNA, miRNA-ncRNA and protein-RNA interaction networks from large-scale CLIP-Seq data. *Nucleic Acids Res*. 2014;42:D92-D97.
46. Zhou G, Soufan O, Ewald J, Hancock REW, Basu N, Xia J. NetworkAnalyst 3.0: a visual analytics platform for comprehensive gene expression profiling and meta-analysis. *Nucleic Acids Res*. 2019;47: W234-W241.
47. Khan A, Fornes O, Stigliani A, et al. JASPAR 2018: update of the open-access database of transcription factor binding profiles and its web framework. *Nucleic Acids Res*. 2018;46:D260-D266.
48. Robin X, Turck N, Hainard A, et al. pROC: an open-source package for R and S+ to analyze and compare ROC curves. *BMC Bioinformatics*. 2011;12:77.
49. Aleissa MM, Silverman EA, Paredes Acosta LM, Nutt CT, Richterman A, Marty FM. New perspectives on antimicrobial agents: remdesivir treatment for COVID-19. *Antimicrob Agents Chemother*. 2020;65:e01814-e01820.
50. Ciancanelli MJ, Huang SX, Luthra P, et al. Infectious disease. Life-threatening influenza and impaired interferon amplification in human IRF7 deficiency. *Science*. 2015;348:448-453.
51. Jin HK, Yoshimatsu K, Takada A, et al. Mouse Mx2 protein inhibits hantavirus but not influenza virus replication. *Arch Virol*. 2001;146:41-49.
52. Koliopoulos MG, Lethier M, van der Veen AG, et al. Molecular mechanism of influenza A NS1-mediated TRIM25 recognition and inhibition. *Nat Commun*. 2018;9:1820.
53. Wu X, Wang J, Wang S, et al. Inhibition of influenza A virus replication by TRIM14 via its multifaceted protein-protein interaction with NP. *Front Microbiol*. 2019;10:344.
54. Rohaim MA, Santhakumar D, Naggar RFE, Iqbal M, Hussein HA, Munir M. Chickens expressing IFIT5 ameliorate clinical outcome and pathology of highly pathogenic avian influenza and velogenic newcastle disease viruses. *Front Immunol*. 2018;9:2025.
55. Feng B, Zhang Q, Wang J, et al. IFIT1 expression patterns induced by H9N2 virus and inactivated viral particle in human umbilical vein endothelial cells and bronchus epithelial cells. *Mol Cells*. 2018;41:271-281.
56. Gad HH, Paulous S, Belarbi E, et al. The E2-E166K substitution restores Chikungunya virus growth in OAS3 expressing cells by acting on viral entry. *Virology*. 2012;434:27-37.
57. Ishibashi M, Wakita T, Esumi M. 2',5'-Oligoadenylate synthetase-like gene highly induced by hepatitis C virus infection in human liver is inhibitory to viral replication in vitro. *Biochem Biophys Res Commun*. 2010;392:397-402.
58. Chen L, Li S, McGilvray I. The ISG15/USP18 ubiquitin-like pathway (ISGylation system) in hepatitis C virus infection and resistance to interferon therapy. *Int J Biochem Cell Biol*. 2011;43:1427-1431.
59. Kurokawa C, Iankov ID, Galanis E. A key anti-viral protein, RSAD2/VIPERIN, restricts the release of measles virus from infected cells. *Virus Res*. 2019;263:145-150.
60. Xia M, Gonzalez P, Li C, et al. Mitophagy enhances oncolytic measles virus replication by mitigating DDX58/RIG-I-like receptor signaling. *J Virol*. 2014;88:5152-5164.
61. Hang do TT, Song JY, Kim MY, Park JW, Shin YK. Involvement of NF-κB in changes of IFN-γ-induced CIITA/MHC-II and iNOS expression by influenza virus in macrophages. *Mol Immunol*. 2011;48:1253-1262.
62. Lai C, Wang K, Zhao Z, et al. C-C Motif Chemokine Ligand 2 (CCL2) Mediates Acute Lung Injury Induced by Lethal Influenza H7N9 Virus. *Front Microbiol*. 2017;8:587.
63. Li W, Wang G, Zhang H, et al. Differential suppressive effect of promyelocytic leukemia protein on the replication of different subtypes/strains of influenza A virus. *Biochem Biophys Res Commun*. 2009;389:84-89.
64. Jiang H, Shen SM, Yin J, Zhang PP, Shi Y. Sphingosine 1-phosphate receptor 1 (S1PR1) agonist CYM5442 inhibits expression of intracellular adhesion molecule 1 (ICAM1) in endothelial cells infected with influenza A viruses. *PLoS ONE*. 2017;12:e0175188.
65. Liu Y, Li S, Zhang G, et al. Genetic variants in IL1A and IL1B contribute to the susceptibility to 2009 pandemic H1N1 influenza A virus. *BMC Immunol*. 2013;14:37.
66. Verhelst J, Parthoens E, Schepens B, Fiers W, Saelens X. Interferon-inducible protein Mx1 inhibits influenza virus by interfering with functional viral ribonucleoprotein complex assembly. *J Virol*. 2012;86:13445-13455.
67. Huipao N, Borwornpinyo S, Wiboon-Ut S, et al. P2Y6 receptors are involved in mediating the effect of inactivated avian influenza virus H5N1 on IL-6 & CXCL8 mRNA expression in respiratory epithelium. *PLoS ONE*. 2017;12:e0176974.
68. Law AH, Lee DC, Yuen KY, Peiris M, Lau AS. Cellular response to influenza virus infection: a potential role for autophagy in CXCL10 and interferon-alpha induction. *Cell Mol Immunol*. 2010;7:263-270.
69. Lee B, Gopal R, Manni ML, et al. STAT1 is required for suppression of type 17 immunity during influenza and bacterial superinfection. *Immunohorizons*. 2017;1:81-91.
70. Warnking K, Klemm C, Löffler B, et al. Super-infection with Staphylococcus aureus inhibits influenza virus-induced type I IFN signalling through impaired STAT1-STAT2 dimerization. *Cell Microbiol*. 2015;17:303-317.
71. Lin X, Yu S, Ren P, Sun X, Jin M. Human microRNA-30 inhibits influenza virus infection by suppressing the expression of SOCS1, SOCS3, and NEDD4. *Cell Microbiol*. 2020;22:e13150.
72. Ren R, Wu S, Cai J, et al. The H7N9 influenza A virus infection results in lethal inflammation in the mammalian host via the NLRP3-caspase-1 inflammasome. *Sci Rep*. 2017;7:7625.
73. Wu W, Zhang W, Duggan ES, Booth JL, Zou MH, Metcalf JP. RIG-I and TLR3 are both required for maximum interferon induction by influenza virus in human lung alveolar epithelial cells. *Virology*. 2015;482:181-188.
74. Ishikawa E, Nakazawa M, Yoshinari M, Minami M. Role of tumor necrosis factor-related apoptosis-inducing ligand in immune response to influenza virus infection in mice. *J Virol*. 2005;79:7658-7663.

75. Wang J, Wang Q, Han T, et al. Soluble interleukin-6 receptor is elevated during influenza A virus infection and mediates the IL-6 and IL-32 inflammatory cytokine burst. *Cell Mol Immunol*. 2015;12:633-644.
76. Di Pietro A, Kajaste-Rudnitski A, Oteiza A, et al. TRIM22 inhibits influenza A virus infection by targeting the viral nucleoprotein for degradation. *J Virol*. 2013;87:4523-4533.
77. Sun X, Zeng H, Kumar A, Belser JA, Maines TR, Tumpey TM. Constitutively expressed IFITM3 protein in human endothelial cells poses an early infection block to human influenza viruses. *J Virol*. 2016;90:11157-11167.
78. Wang K, Lai C, Gu H, et al. miR-194 inhibits innate antiviral immunity by targeting FGF2 in influenza H1N1 virus infection. *Front Microbiol*. 2017;8:2187.
79. Yu M, Qi W, Huang Z, et al. Expression profile and histological distribution of IFITM1 and IFITM3 during H9N2 avian influenza virus infection in BALB/c mice. *Med Microbiol Immunol*. 2015;204:505-514.
80. Wang HF, Chen L, Luo J, He HX. KLF5 is involved in regulation of IFITM1, 2, and 3 genes during H5N1 virus infection in A549 cells. *Cell Mol Biol (Noisy-le-grand)*. 2016;62:65-70.
81. Tang BM, Shojaei M, Parnell GP, et al. A novel immune biomarker IFI27 discriminates between influenza and bacteria in patients with suspected respiratory infection. *Eur Respir J*. 2017;49:1602098.
82. Sanyal S, Ashour J, Maruyama T, et al. Type I interferon imposes a TSG101/ISG15 checkpoint at the Golgi for glycoprotein trafficking during influenza virus infection. *Cell Host Microbe*. 2013;14:510-521.
83. Ye S, Lowther S, Stambas J. Inhibition of reactive oxygen species production ameliorates inflammation induced by influenza A viruses via upregulation of SOCS1 and SOCS3. *J Virol*. 2015;89:2672-2683.
84. Kuriakose T, Zheng M, Neale G, Kanneganti TD. IRF1 is a transcriptional regulator of ZBP1 promoting NLRP3 inflammasome activation and cell death during influenza virus infection. *J Immunol*. 2018;200:1489-1495.
85. Chai W, Li J, Shangguan Q, et al. Lnc-ISG20 inhibits influenza A virus replication by enhancing ISG20 expression. *J Virol*. 2018;92:e00539-e00518.
86. Hebert KD, Mclaughlin N, Zhang Z, Cipriani A, Alcorn JF, Pociask DA. IL-22Ra1 is induced during influenza infection by direct and indirect TLR3 induction of STAT1. *Respir Res*. 2019;20:184.
87. Kedzierski L, Tate MD, Hsu AC, et al. Suppressor of cytokine signaling (SOCS)5 ameliorates influenza infection via inhibition of EGFR signaling. *Elife*. 2017;6:e20444.
88. Feng J, Cao Z, Wang L, et al. Inducible GBP5 mediates the antiviral response via interferon-related pathways during influenza A virus infection. *J Innate Immun*. 2017;9:419-435.
89. Londrigan SL, Tate MD, Job ER, et al. Endogenous murine BST-2/tetherin is not a major restriction factor of influenza A virus infection. *PLoS ONE*. 2015;10:e0142925.
90. Tang Y, Zhong G, Zhu L, et al. Herc5 attenuates influenza A virus by catalyzing ISGylation of viral NS1 protein. *J Immunol*. 2010;184:5777-5790.
91. Kumar P, Rajasekaran K, Nanbakhsh A, Gorski J, Thakar MS, Malarkannan S. IL-27 promotes NK cell effector functions via Maf-Nrf2 pathway during influenza infection. *Sci Rep*. 2019;9:4984.
92. Rangel-Moreno J, Moyron-Quiroz JE, Hartson L, Kusser K, Randall TD. Pulmonary expression of CXC chemokine ligand 13, CC chemokine ligand 19, and CC chemokine ligand 21 is essential for local immunity to influenza. *Proc Natl Acad Sci U S A*. 2007;104:10577-10582.
93. Carlin LE, Hemann EA, Zacharias ZR, Heusel JW, Legge KL. Natural killer cell recruitment to the lung during influenza A virus infection is dependent on CXCR3, CCR5, and virus exposure dose. *Front Immunol*. 2018;9:781.
94. Dai J, Gu L, Su Y, et al. Inhibition of curcumin on influenza A virus infection and influenzal pneumonia via oxidative stress, TLR2/4, p38/JNK MAPK and NF-κB pathways. *Int Immunopharmacol*. 2018;54:177-187.
95. Maelfait J, Roose K, Bogaert P, et al. A20 (Tnfaip3) deficiency in myeloid cells protects against influenza A virus infection. *Plos Pathog*. 2012;8:e1002570.
96. Salimi V, Ramezani A, Mirzaei H, et al. Evaluation of the expression level of 12/15 lipoxygenase and the related inflammatory factors (CCL5, CCL3) in respiratory syncytial virus infection in mice model. *Microb Pathog*. 2017;109:209-213.
97. Ermers MJ, Janssen R, Onland-Moret NC, et al. IL10 family member genes IL19 and IL20 are associated with recurrent wheeze after respiratory syncytial virus bronchiolitis. *Pediatr Res*. 2011;70:518-523.
98. Al-Afif A, Alyazidi R, Oldford SA, et al. Respiratory syncytial virus infection of primary human mast cells induces the selective production of type I interferons, CXCL10, and CCL4. *J Allergy Clin Immunol*. 2015;136:1346-1354.
99. Shi T, He Y, Sun W, et al. Respiratory Syncytial virus infection compromises asthma tolerance by recruiting interleukin-17A-producing cells via CCR6-CCL20 signaling [published correction appears in Mol Immunol. 2018 Jan;93:285]. *Mol Immunol*. 2017;88:45-57.
100. Ternette N, Wright C, Kramer HB, Altun M, Kessler BM. Label-free quantitative proteomics reveals regulation of interferon-induced protein with tetratricopeptide repeats 3 (IFIT3) and 5'-3'-exoribonuclease 2 (XRN2) during respiratory syncytial virus infection. *Virol J*. 2011;8:442.
101. Touzelet O, Broadbent L, Armstrong SD, et al. The secretome profiling of a pediatric airway epithelium infected with hRSV identified aberrant apical/basolateral trafficking and novel immune modulating (CXCL6, CXCL16, CSF3) and antiviral (CEACAM1) proteins. *Mol Cell Proteomics*. 2020;19:793-807.
102. Inchley CS, Osterholt HC, Sonerud T, Fjærli HO, Nakstad B. Downregulation of IL7R, CCR7, and TLR4 in the cord blood of children with respiratory syncytial virus disease. *J Infect Dis*. 2013;208:1431-1435.
103. Conti P, Ronconi G, Caraffa AL, et al. Induction of pro-inflammatory cytokines (IL-1 and IL-6) and lung inflammation by Coronavirus-19 (COVI-19 or SARS-CoV-2): anti-inflammatory strategies. *J Biol Regul Homeost Agents*. 2020;34:327-331.
104. Wu D, Yang XO. TH17 responses in cytokine storm of COVID-19: an emerging target of JAK2 inhibitor Fedratinib. *J Microbiol Immunol Infect*. 2020;53:368-370.
105. Oshiumi H, Okamoto M, Fujii K, et al. The TLR3/TICAM-1 pathway is mandatory for innate immune responses to poliovirus infection. *J Immunol*. 2011;187:5320-5327.
106. Lim JK, Lisco A, McDermott DH, et al. Genetic variation in OAS1 is a risk factor for initial infection with West Nile virus in man. *PLoS Pathog*. 2009;5:e1000321.
107. García-Álvarez M, Berenguer J, Jiménez-Sousa MA, et al. Mx1, OAS1 and OAS2 polymorphisms are associated with the severity of liver disease in HIV/HCV-coinfected patients: a cross-sectional study. *Sci Rep*. 2017;7:41516.
108. Huang W, Hu K, Luo S, et al. Herpes simplex virus type 2 infection of human epithelial cells induces CXCL9 expression and CD4+ T cell migration via activation of p38-CCAAT/enhancer-binding protein-β pathway. *J Immunol*. 2012;188:6247-6257.
109. Ding X, Wang F, Duan M, Yang J, Wang S. Epiregulin as a key molecule to suppress hepatitis B virus propagation in vitro. *Arch Virol*. 2009;154:9-17.
110. Riezu-Boj JI, Larrea E, Aldabe R, et al. Hepatitis C virus induces the expression of CCL17 and CCL22 chemokines that attract regulatory T cells to the site of infection. *J Hepatol*. 2011;54:422-431.
111. Koraka P, Murgue B, Deparis X, et al. Elevation of soluble VCAM-1 plasma levels in children with acute dengue virus infection of varying severity. *J Med Virol*. 2004;72:445-450.
112. Das A, Dinh PX, Panda D, Pattnaik AK. Interferon-inducible protein IFI35 negatively regulates RIG-I antiviral signaling and supports vesicular stomatitis virus replication. *J Virol*. 2014;88:3103-3113.
113. Fensterl V, Wetzel JL, Sen GC. Interferon-induced protein Ifit2 protects mice from infection of the peripheral nervous system by vesicular stomatitis virus. *J Virol*. 2014;88:10303-10311.
114. Berthoux L, Sebastian S, Sokolskaja E, Luban J. Cyclophilin A is required for TRIM5{alpha}-mediated resistance to HIV-1 in Old World monkey cells. *Proc Natl Acad Sci U S A*. 2005;102:14849-14853.
115. Long X, Li Y, Qi Y, et al. XAF1 contributes to dengue virus-induced apoptosis in vascular endothelial cells. *FASEB J*. 2013;27:1062-1073.
116. Chen S, Li S, Chen L. Interferon-inducible Protein 6-16 (IFI-6-16, ISG16) promotes Hepatitis C virus replication in vitro. *J Med Virol*. 2016;88:109-114.
117. Levy Y, Lacabaratz C, Weiss L, et al. Enhanced T cell recovery in HIV-1-infected adults through IL-7 treatment. *J Clin Invest*. 2009;119:997-1007.
118. Kim YE, Lee JH, Kim ET, et al. Human cytomegalovirus infection causes degradation of Sp100 proteins that suppress viral gene expression. *J Virol*. 2011;85:11928-11937.
119. Pan W, Zuo X, Feng T, Shi X, Dai J. Guanylate-binding protein 1 participates in cellular antiviral response to dengue virus. *Virol J*. 2012;9:292.
120. Fukutani ER, Ramos PI, Kasprzykowski JI, et al. Meta-analysis of HTLV-1-infected patients identifies CD40LG and GBP2 as markers of ATLL and HAM/TSP clinical status: two genes beat as one. *Front Genet*. 2019;10:1056.
121. Grusdat M, McIlwain DR, Xu HC, et al. IRF4 and BATF are critical for CD8^{+} T-cell function following infection with LCMV. *Cell Death Differ*. 2014;21:1050-1060.
122. Khlaiphuengsin A, T-Thienprasert NP, Tangkijvanich P, et al. Human miR-5193 triggers gene silencing in multiple genotypes of hepatitis B virus. *Microrna*. 2015;4:123-130.
123. Manuel O, Wójtowicz A, Bibert S, et al. Influence of IFNL3/4 polymorphisms on the incidence of cytomegalovirus infection after solid-organ transplantation. *J Infect Dis*. 2015;211:906-914.
124. Malikova J, Zingg T, Fingerhut R, et al. HIV drug efavirenz inhibits CYP21A2 activity with possible clinical implications. *Horm Res Paediatr*. 2019;91:262-270.
125. Guha D, Klamar CR, Reinhart T, Ayyavoo V. Transcriptional regulation of CXCL5 in HIV-1-infected macrophages and its functional consequences on CNS pathology. *J Interferon Cytokine Res*. 2015;35:373-384.
126. Bertin J, Jalaguier P, Barat C, Roy MA, Tremblay MJ. Exposure of human astrocytes to leukotriene C4 promotes a CX3CL1/fractalkine-mediated transmigration of HIV-1-infected CD4^{+} T cells across an in vitro blood-brain barrier model. *Virology*. 2014;454-455:128-138.
127. Shao W, Tang J, Song W, et al. CCL3L1 and CCL4L1: variable gene copy number in adolescents with and without human immunodeficiency virus type 1 (HIV-1) infection. *Genes Immun*. 2007;8:224-231.

128. Xie L, Huang Y, Zhong J, et al. Short communication: the association of WNT16 polymorphisms with the CD4+ T cell count in the HIV-infected population. *AIDS Res Hum Retroviruses*. 2020;36:119-121.
129. Juno J, Tuff J, Choi R, et al. The role of G protein gene GNB3 C825T polymorphism in HIV-1 acquisition, progression and immune activation. *Retrovirology*. 2012;9:1.
130. Oyoshi MK, Beaupré J, Venturelli N, Lewis CN, Iwakura Y, Geha RS. Filaggrin deficiency promotes the dissemination of cutaneously inoculated vaccinia virus. *J Allergy Clin Immunol*. 2015;135:1511-1518.
131. Wang X, He Z, Xia T, et al. Latency-associated nuclear antigen of Kaposi sarcoma-associated herpesvirus promotes angiogenesis through targeting notch signaling effector Hey1. *Cancer Res*. 2014;74:2026-2037.
132. Sanders SP, Siekierski ES, Richards SM, Porter JD, Imani F, Proud D. Rhinovirus infection induces expression of type 2 nitric oxide synthase in human respiratory epithelial cells in vitro and in vivo. *J Allergy Clin Immunol*. 2001;107:235-243.
133. Bonville CA, Lau VK, DeLeon JM, et al. Functional antagonism of chemokine receptor CCR1 reduces mortality in acute pneumovirus infection in vivo. *J Virol*. 2004;78:7984-7989.
134. Liu H, Yang X, Zhang ZK, Zou WC, Wang HN. miR-146a-5p promotes replication of infectious bronchitis virus by targeting IRAK2 and TNFRSF18. *Microb Pathog*. 2018;120:32-36.
135. Wheeler LA, Trifonova RT, Vrbanac V, et al. TREX1 knockdown induces an interferon response to HIV that delays viral infection in humanized mice. *Cell Rep*. 2016;15:1715-1727.
136. O'Brien TR, Pfeiffer RM, Paquin A, et al. Comparison of functional variants in IFNL4 and IFNL3 for association with HCV clearance. *J Hepatol*. 2015;63:1103-1110.
137. Libraty DH, Zhang L, Obcena A, Brion JD, Capeding RZ. Circulating levels of soluble MICB in infants with symptomatic primary dengue virus infections. *PLoS ONE*. 2014;9:e98509.
138. Zenner HL, Yoshimura S, Barr FA, Crump CM. Analysis of Rab GTPase-activating proteins indicates that Rab1a/b and Rab43 are important for herpes simplex virus 1 secondary envelopment. *J Virol*. 2011;85:8012-8021.
139. Estrella MM, Li M, Tin A, et al. The association between APOL1 risk alleles and longitudinal kidney function differs by HIV viral suppression status. *Clin Infect Dis*. 2015;60:646-652.
140. Orzalli MH, Broekema NM, Diner BA, et al. cGAS-mediated stabilization of IFI16 promotes innate signaling during herpes simplex virus infection. *Proc Natl Acad Sci U S A*. 2015;112:E1773-E1781.
141. Kim EY, Lorenzo-Redondo R, Little SJ, et al. Human APOBEC3 induced mutation of human immunodeficiency virus type-1 contributes to adaptation and evolution in natural infection. *PLoS Pathog*. 2014;10:e1004281.
142. O'Connell P, Pepelyayeva Y, Blake MK, et al. SLAMF7 is a critical negative regulator of IFN-α-mediated CXCL10 production in chronic HIV infection. *J Immunol*. 2019;202:228-238.
143. Chen J, Wang N, Dong M, et al. The metabolic regulator histone deacetylase 9 contributes to glucose homeostasis abnormality induced by hepatitis C virus infection. *Diabetes*. 2015;64:4088-4098.
144. Berger G, Durand S, Fargier G, et al. APOBEC3A is a specific inhibitor of the early phases of HIV-1 infection in myeloid cells. *PLoS Pathog*. 2011;7:e1002221.
145. Sanfilippo C, Cambria D, Longo A, et al. SERPING1 mRNA overexpression in monocytes from HIV+ patients. *Inflamm Res*. 2017;66:1107-1116.
146. Soundravally R, Hoti SL. Significance of transporter associated with antigen processing 2 (TAP2) gene polymorphisms in susceptibility to dengue viral infection. *J Clin Immunol*. 2008;28:256-262.
147. Tian X, Zhang A, Qiu C, et al. The upregulation of LAG-3 on T cells defines a subpopulation with functional exhaustion and correlates with disease progression in HIV-infected subjects. *J Immunol*. 2015;194:3873-3882.
148. Waisner H, Kalamvoki M. The ICP0 Protein of Herpes Simplex Virus 1 (HSV-1) Downregulates major autophagy adaptor proteins sequestosome 1 and optineurin during the early stages of HSV-1 infection. *J Virol*. 2019;93:e01258-e01219.
149. McGuinness PH, Painter D, Davies S, McCaughan GW. Increases in intrahepatic CD68 positive cells, MAC387 positive cells, and proinflammatory cytokines (particularly interleukin 18) in chronic hepatitis C infection. *Gut*. 2000;46:260-269.
150. Madani N, Millette R, Platt EJ, et al. Implication of the lymphocyte-specific nuclear body protein Sp140 in an innate response to human immunodeficiency virus type 1. *J Virol*. 2002;76:11133-11138.
151. Nasi M, Riva A, Borghi V, et al. Novel genetic association of TNF-α-238 and PDCD1-7209 polymorphisms with long-term non-progressive HIV-1 infection. *Int J Infect Dis*. 2013;17:e845-e850.
152. Tse D, Armstrong DA, Oppenheim A, Kuksin D, Norkin L, Stan RV. Plasmalemmal vesicle associated protein (PV1) modulates SV40 virus infectivity in CV-1 cells. *Biochem Biophys Res Commun*. 2011;412:220-225.
153. Fahrbach KM, Barry SM, Ayehunie S, Lamore S, Klausner M, Hope TJ. Activated CD34-derived Langerhans cells mediate transinfection with human immunodeficiency virus. *J Virol*. 2007;81:6858-6868.
154. Benito JM, López M, Lozano S, Martinez P, González-Lahoz J, Soriano V. CD38 expression on CD8 T lymphocytes as a marker of residual virus replication in chronically HIV-infected patients receiving antiretroviral therapy. *AIDS Res Hum Retroviruses*. 2004;20:227-233.
155. Yong YK, Tan HY, Saeidi A, et al. Decrease of CD69 levels on TCR Vα7.2+CD4+ innate-like lymphocytes is associated with impaired cytotoxic functions in chronic hepatitis B virus-infected patients. *Innate Immun*. 2017;23:459-467.
156. Pineda-Tenor D, Micheloud D, Berenguer J, et al. SLC30A8 rs13266634 polymorphism is related to a favorable cardiometabolic lipid profile in HIV/hepatitis C virus-coinfected patients. *AIDS*. 2014;28:1325-1332.
157. Shichi D, Kikkawa EF, Ota M, et al. The haplotype block, NFKBIL1-ATP6V1G2-BAT1-MICB-MICA, within the class III-class I boundary region of the human major histocompatibility complex may control susceptibility to hepatitis C virus-associated dilated cardiomyopathy. *Tissue Antigens*. 2005;66:200-208.
158. Pauli EK, Schmolke M, Hofmann H, et al. High level expression of the antiretroviral protein APOBEC3G is induced by influenza A virus but does not confer antiviral activity. Retrovirology. 2009;6:38.
159. Ma GF, Miettinen S, Porola P, Hedman K, Salo J, Konttinen YT. Human parainfluenza virus type 2 (HPIV2) induced host ADAM8 expression in human salivary adenocarcinoma cell line (HSY) during cell fusion. *BMC Microbiol*. 2009;9:55.
160. Zhang T, Yin C, Boyd DF, et al. Influenza virus Z-RNAs induce ZBP1-mediated necroptosis. *Cell*. 2020;180:1115-1129.e13.
161. Ranjan P, Singh N, Kumar A, et al. NLRC5 interacts with RIG-I to induce a robust antiviral response against influenza virus infection. *Eur J Immunol*. 2015;45:758-772.
162. Zhang H, Luo J, Alcorn JF, et al. AIM2 inflammasome is critical for influenza-induced lung injury and mortality. *J Immunol*. 2017;198:4383-4393.
163. Kim BJ, Cho SW, Jeon YJ, et al. Intranasal delivery of Duox2 DNA using cationic polymer can prevent acute influenza A viral infection in vivo lung. *Appl Microbiol Biotechnol*. 2018;102:105-115.
164. Selemidis S, Seow HJ, Broughton BR, et al. Nox1 oxidase suppresses influenza a virus-induced lung inflammation and oxidative stress. *PLoS ONE*. 2013;8:e60792.
165. Fox JM, Crabtree JM, Sage LK, Tompkins SM, Tripp RA. Interferon lambda upregulates IDO1 expression in respiratory epithelial cells after influenza virus infection. *J Interferon Cytokine Res*. 2015;35:554-562.
166. Ye S, Cowled CJ, Yap CH, Stambas J. Deep sequencing of primary human lung epithelial cells challenged with H5N1 influenza virus reveals a proviral role for CEACAM1. *Sci Rep*. 2018;8:15468.
167. Job ER, Bottazzi B, Short KR, et al. A single amino acid substitution in the hemagglutinin of H3N2 subtype influenza A viruses is associated with resistance to the long pentraxin PTX3 and enhanced virulence in mice. *J Immunol*. 2014;192:271-281.
168. Asp L, Holtze M, Powell SB, Karlsson H, Erhardt S. Neonatal infection with neurotropic influenza A virus induces the kynurenine pathway in early life and disrupts sensorimotor gating in adult Tap1-/- mice. *Int J Neuropsychopharmacol*. 2010;13:475-485.
169. Wang G, Jiang L, Wang J, et al. The G protein-coupled receptor FFAR2 promotes internalization during influenza A virus entry. *J Virol*. 2020;94:e01707-e01719.
170. Mayank AK, Sharma S, Nailwal H, Lal SK. Nucleoprotein of influenza A virus negatively impacts antiapoptotic protein API5 to enhance E2F1-dependent apoptosis and virus replication. *Cell Death Dis*. 2015;6:e2018.
171. Chen X, Zhang Q, Bai J, et al. The nucleocapsid protein and nonstructural protein 10 of highly pathogenic porcine reproductive and respiratory syndrome virus enhance CD83 production via NF-κB and Sp1 signaling pathways. *J Virol*. 2017;91:e00986-e00917.
172. Hoffmann M, Kleine-Weber H, Schroeder S, et al. SARS-CoV-2 cell entry depends on ACE2 and TMPRSS2 and is blocked by a clinically proven protease inhibitor. *Cell*. 2020;181:271-280.e8.
173. Cheng W, Chen S, Li R, Chen Y, Wang M, Guo D. Severe acute respiratory syndrome coronavirus protein 6 mediates ubiquitin-dependent proteosomal degradation of N-Myc (and STAT) interactor. *Virol Sin*. 2015;30:153-161.
174. Seyerl M, Kirchberger S, Majdic O, et al. Human rhinoviruses induce IL-35-producing Treg via induction of B7-H1 (CD274) and sialoadhesin (CD169) on DC. *Eur J Immunol*. 2010;40:321-329.
175. Fusco DN, Pratt H, Kandilas S, et al. HELZ2 is an IFN effector mediating suppression of dengue virus. *Front Microbiol*. 2017;8:240. doi:10.3389/fmicb.2017.00240.
176. Desai P, Tahiliani V, Abboud G, Stanfield J, Salek-Ardakani S. Batf3-dependent dendritic cells promote optimal CD8 T cell responses against respiratory poxvirus infection. *J Virol*. 2018;92:e00495-18.
177. Uckun FM, Chelstrom LM, Tuel-Ahlgren L, et al. TXU (anti-CD7)-pokeweed antiviral protein as a potent inhibitor of human immunodeficiency virus. *Antimicrob Agents Chemother*. 1998;42:383-388.
178. Purdy JG, Shenk T, Rabinowitz JD. Fatty acid elongase 7 catalyzes lipidome remodeling essential for human cytomegalovirus replication. *Cell Rep*. 2015;10:1375-1385.